REPORT DOCUMENTATION PAGE

Form Approved
OMB No. 0704-0188

1. REPORT DATE (DD-MM-YY)	2. REPORT TYPE	3. DATES COVERED (From – To)
15-09-2010	Technical Report	

4. TITLE AND SUBTITLE

Crimp-Imbalanced Protective (CRIMP) Fabrics: An Analytical Investigation into the Relationship between Crimp Contents, Energy Absorption, and Fabric Ballistic Performance

5a. CONTRACT NUMBER
MIPR 8HDAVBW332

5b. GRANT NUMBER

5c. PROGRAM ELEMENT NUMBER

6. AUTHOR(S)

Ali M. Sadegh
Paul V. Cavallaro

5.d PROJECT NUMBER

5e. TASK NUMBER

5f. WORK UNIT NUMBER

7. PERFORMING ORGANIZATION NAME(S) AND ADDRESS(ES)

Naval Undersea Warfare Center Division
1176 Howell Street
Newport, RI 02841-1708

8. PERFORMING ORGANIZATION REPORT NUMBER

TR 11, 970

9. SPONSORING/MONITORING AGENCY NAME(S) AND ADDRESS(ES)

Army Research Laboratory's Weapons & Materials Directorate
Aberdeen Proving Grounds, MD 21005-5069

10. SPONSORING/MONITOR'S ACRONYM

ARLWMD

11. SPONSORING/MONITORING REPORT NUMBER

12. DISTRIBUTION/AVAILABILITY STATEMENT

Approved for public release; distribution is unlimited.

13. SUPPLEMENTARY NOTES

14. ABSTRACT

This report documents research that was conducted to analytically investigate the relationships between dynamic energy absorption of plain-woven fabrics commonly used in protective systems and the architectural parameters used to describe their construction including, for example, crimp contents, yarn density ratios, and yarn-yarn friction. The research results showed that for plain-woven fabrics subject to ballistic impacts, highly crimp-imbalanced, plain-woven fabrics performed in a manner far superior to that of crimp-balanced, plain- woven fabrics. These analytical solutions resulted in the ability to parametrically study the effect of crimp imbalance on the dynamic energy absorbability of plain-woven fabrics.

15. SUBJECT TERMS

Fabric Armor Textiles | Crimp Woven Fabrics | Crimp Interchange | Ballistic Impact | Energy Absorption | Fragment Protection

16. SECURITY CLASSIFICATION OF:			17. LIMITATION OF ABSTRACT	18. NUMBER OF PAGES	19a. NAME OF RESPONSIBLE PERSON
a. REPORT	b. ABSTRACT	c. THIS PAGE			Paul V. Cavallaro
Unclassified	Unclassified	Unclassified	SAR	46	19b. TELEPHONE NUMBER (Include area code) 401-832-5082

NUWC-NPT Technical Report 11,970
15 September 2010

Crimp-Imbalanced Protective (CRIMP) Fabrics: An Analytical Investigation into the Relationship Between Crimp Contents, Energy Absorption, and Fabric Ballistic Performance

Ali M. Sadegh
Paul V. Cavallaro
Ranges, Engineering, and Analysis Department

Naval Undersea Warfare Center Division
Newport, Rhode Island

PREFACE

This report was funded under NUWC Division Newport Assignment Number TD0207, principal investigator Paul V. Cavallaro (Code 702). The research was sponsored by the Army Research Laboratory's Weapons & Materials Directorate (ARL-WMD), Aberdeen Proving Grounds, MD, through Military Interagency Purchase Request Number 8HDAVBW332. The sponsoring officer was Robert B. Dooley.

The authors gratefully acknowledge Robert B. Dooley and Bryan A. Cheeseman of ARL-WMD for their support. Special thanks are given to Charles Howland of Warwick Mills, New Ipswich, NH, for sharing his technical expertise in yarn materials, ballistic fabric constructions, and textile manufacturing.

The technical reviewer was Andrew J. Hull (Code 8212).

Reviewed and Approved: 15 September 2010

Harriet L. Coleman

Harriet L. Coleman
Head, Ranges, Engineering, and Analysis Department

TABLE OF CONTENTS

Page

LIST OF ILLUSTRATIONS

LIST OF ILLUSTRATIONS (Cont'd)

Figure **Page**

LIST OF ABBREVIATIONS, ACRONYMS, AND SYMBOLS

a	Amplitude of cosine distributed load
CRIMP	Crimp-imbalanced protective fabric
F_i	Projectile force on yarn
h	Distance between the centerlines of adjacent crossover regions in the HCC yarn direction
HCC	High crimp content
LCC	Low crimp content
N	Newton
n	Number of crossover regions
P	$P = R/T_n$
r	Radius of yarn cross-section
R	Yarn migration force
RCC	Right circular cylinder
t	Distance between the centerlines of adjacent crossover regions in the LCC yarn direction
T_i	Yarn pullout (tension) force

LIST OF ABBREVIATIONS, ACRONYMS, AND SYMBOLS (Cont'd)

T_n	Tension at clamped side of fabric
V_1	Initial projectile velocity
V_2	Residual projectile velocity
YDR	Yarn density ratio
ω	Uniform load per unit length
μ	Coefficient of friction
α	Contact angle of the yarns at a crossover region
θ	Circumferential contact angle
δ	Deflection

CRIMP-IMBALANCED PROTECTIVE (CRIMP) FABRICS: AN ANALYTICAL INVESTIGATION INTO THE RELATIONSHIP BETWEEN CRIMP CONTENTS, ENERGY ABSORPTION, AND FABRIC BALLISTIC PERFORMANCE

INTRODUCTION

PURPOSE

Modifications to current woven fabric architectures are being investigated to further establish and potentially improve the ballistic impact resistance of flexible protection systems constructed with high-performance fibers. The authors' most recent numerical study[1] documents an investigation that explored using crimp imbalance as a mechanism to enhance fragmentation and ballistic protection levels of single-ply, plain-woven fabrics. Prior to this study, the influence of yarn crimp on the ballistic impact resistance of plain-woven fabrics had neither been sufficiently addressed nor adequately understood; the open literature lacked conclusive research findings relating yarn crimp to energy absorption levels. The authors' findings demonstrated that crimp imbalance (defined using the ratio of crimp contents among yarn directions) had substantial influence on the energy absorption levels of single-ply, plain-woven fabrics. This current investigation, an extension of their earlier research,[1] describes a series of analytical models developed to establish the relationship between crimp imbalance and the dynamic energy absorbability of plain-woven fabrics subjected to ballistic impact.

Specifically, the primary objectives of this research were to (1) investigate the projectile penetration mechanisms in single-ply, plain-woven fabrics, (2) develop analytical solutions of yarn pullout force, (3) compute the work required to create openings between yarns through yarn migration, and (4) to determine the energy absorbed by a projectile when it passes through these openings. This research showed that, for ballistic impacts in single-ply, plain-woven fabrics, the performance of highly crimp-imbalanced woven architectures was superior to that of crimp-balanced woven architectures. The analytical solutions provide the means to parametrically quantify the effects of crimp imbalance on the protection levels of fabric armor materials.

BACKGROUND

Flexible woven fabrics remain outstanding material systems for lightweight protection against ballistic and fragment impacts. Because of their heterogeneous constructions on multiple scales, these fabrics can absorb significant kinetic energy from projectile and fragment impacts through a combination of design factors, including yarn material, weaving architecture, yarn density ratio (that is, the ratio of yarn counts per unit length), as well as the projectile size, shape, and velocity.[2,3,4] The mechanisms responsible for energy absorbability in plain-woven fabrics include yarn friction, crimp interchange, yarn stretching, yarn migration, fabric shearing, yarn pullout, and yarn breakage.[5,6] While the mechanisms of energy absorbability in fabrics have

been recognized, their relationships to ballistic protection levels have not been fully quantified in the open literature.

A normal impact between a projectile and plain-woven fabric causes the following sequence of events to occur: (1) the projectile creates a conical depression on the plane of the fabric upon initial contact; (2) the yarns that are in direct contact with the projectile (referred to as "primary yarns") are subjected to tension, and, at the crossover regions where yarn families intersect, shearing deformations develop; and (3) primary yarns begin to migrate away from the projectile contact region. The energy absorbed by the fabric depends on the mass, velocity, and impact force of the projectile; the fabric architecture and yarn construction; and on the material properties of the fibers.

Forces due to projectile impacts can be classified into two categories: high-velocity impacts and low-velocity impacts. In high-velocity ballistic impacts where the projectile velocity exceeds 300 m/sec, the yarns may fail prior to the occurrence of yarn migration. In low-velocity ballistic impacts, a woven fabric may absorb the projectile's kinetic energy through the following sequential phenomena: (1) global (overall) conical deflection of the fabric, (2) friction at the crossover regions, (3) crimp interchange (a biaxial phenomenon) caused by yarn tensions, (4) yarn migration away from the impact zone, (5) fabric shearing, and (6) out-of-plane extraction of yarns from within the fabric yarns. This sequence of events can be sufficient to create openings, enabling the projectile to penetrate the fabric without yarn failure. The analysis described in this report invokes the following assumptions: (1) the impact velocity is considered to be within the low-velocity regime and (2) the yarns do not fail, rather, they are permitted to migrate with respect to each other.

SCOPE

Contrary to the intuitive belief that tightly woven and equally crimped (also referred to as "iso-crimped") fabrics perform well in ballistic impacts, it has been argued and demonstrated that highly crimp-imbalanced woven fabrics can perform in a manner far superior to iso-crimped woven fabrics.[1] This research analytically investigates the validity of such a claim. Specifically, this work focuses on energy absorption of a fabric (that is, the reduction of projectile velocity upon impact) as a function of the contact angle α (that is, the angle of circumferential contact between crossing yarns). Note that the magnitude of α constitutes the crimp ratio and the crimp imbalance.

In short, this research investigates the energy absorbability of a yarn in a crimp-imbalanced protective (CRIMP) fabric when subjected to a ballistic impact force. Specific areas of investigation include (1) a closed-form approach to analytically investigate the associated parametric effects of crimp content and friction on the energy absorbability resulting from a projectile impacting a plain-woven fabric, (2) woven fabric architecture, (3) yarn migration, (4) yarn pullout, and (5) energy absorption and projectile residual velocity.

FRICTION PHENOMENON

To understand the energy absorbability of woven fabric targets, one must consider the kinematic, elastic, plastic, viscoelastic, and dissipative mechanisms associated with individual yarns and their interactions. These mechanisms involve the occurrence of yarn decrimping, yarn stretching, yarn migration, and yarn pullout—all of which must be investigated. The forces required for yarn migration and pullout are related to the frictional properties of the yarns. The ballistic protection levels of woven fabrics can be greatly altered, and often enhanced, by modifications to the frictional properties at both the fiber and yarn levels.[7,8,9]

During projectile impact with a woven fabric, several frictional forces are generated, the first of which is the frictional force between the projectile and the fabric. This force is negligible on metallic plates, as demonstrated by experimental work of Awerbuch and Bodner,[10] and will be assumed negligible in the present fabric cases. The second frictional force arises from friction developed between fabric layers in a multilayered fabric system which is not considered here in the singly-ply fabric cases. The third frictional force results from the friction between yarn families at the crossover regions; it is this frictional force that plays an important role in energy absorbability.

FRICTION AT A CROSSOVER REGION

Consider a single crossover region where the superior (primary) yarn wraps over the crossing yarn. Using the basic mechanics of rope around a cylinder (figure 1) and equilibrium of forces on a small sector of the rope (figure 2), the ratio of the tensions (T_1/T_2) on either side of the crossover region is written as

$$\frac{T_1}{T_2} = e^{\mu\theta}, \tag{1}$$

where μ is the yarn-to-yarn coefficient of friction and θ is the circumferential contact angle.

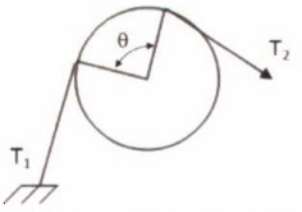

Figure 1. Representation of the Ratio of Tension in a Yarn at a Crossover Region

When a projectile contacts a woven fabric, it applies a contact force on several crossover regions. Consider a crossover region subjected to a contact force as shown in figure 2. Depending on the shape of the leading surface of the projectile, this force could be described by a uniform load or a cosine-shaped load (figure 3). The contact force creates three distinct sectors on the crossover region: α_1, α_2, and α_3. Let $\alpha = \alpha_1 + \alpha_2 + \alpha_3$. Note that α_2 is the sector where the

projectile contacts the crossing yarn (see figure 3). Two angles β_1 and β_2 were introduced so that $\beta_1 + \alpha_1 + \alpha_2 + \alpha_3 + \beta_2 = 180°$. Because of the symmetric loading of the crown of the crossover region, $\alpha_1 = \alpha_3$ and $\beta_1 = \beta_2$. Note that $\beta_1 = \beta_2 = \frac{180 - \alpha}{2}$. Although α_1 and α_3 and β_1 and β_2 are small compared to α_2, the yarn tensions on sectors α_1 and α_3 are nevertheless denoted as T_3 and T_2, respectively, which are different values than those of T_1 and T_4. When $\alpha_1 = \alpha_3 = 0$, then $T_3 = T_4$ and $T_1 = T_2$.

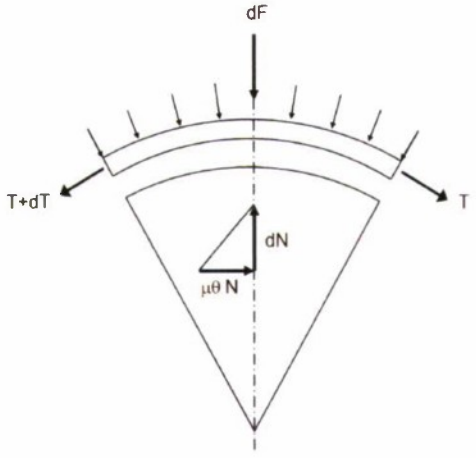

Figure 2. Free-Body Diagram of the Yarn at a Crossover Region

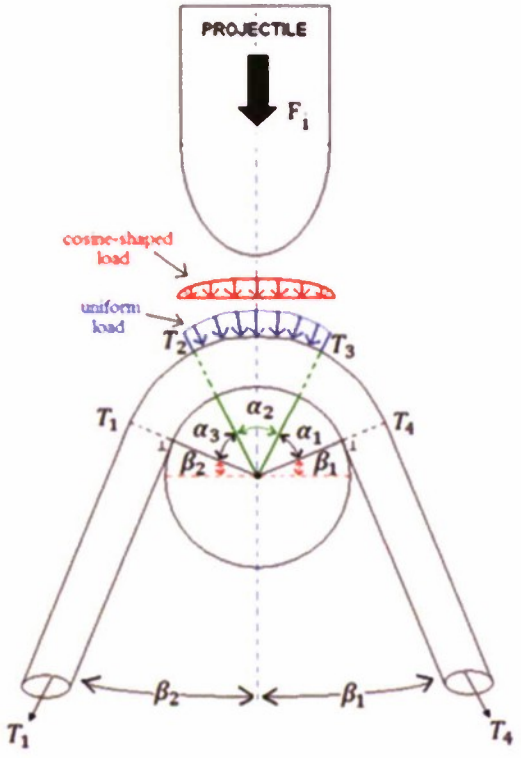

Figure 3. Projectile Force and Geometry at a Crossover Region (Uniform and Cosine-Shaped Loads)

Uniformly Distributed Load

Consider a uniformly distributed load, ω, per unit length that resides over the angle α_2 (see figure 3). The total applied force to the i^{th} crossover region is denoted by $F_i = \omega r \alpha_2$, where r is the radius of the yarn. Three contact sections exist along the crossing yarn. The first and the third contact regions over the sectors α_1 and α_3 are governed by the basic friction equation (1) and are shown in equations (2) and (4); the second contact region over sector α_2 was derived, following the equation of a sector shown in figure 2 and is given in equation (3). Solving the coupled equations (2) to (4), the ratio of T_1/T_4 can be calculated:

$$\frac{T_3}{T_4} = e^{\mu\alpha_1}, \tag{2}$$

$$\frac{T_2 + \dfrac{F_i}{\alpha_2}}{T_3 + \dfrac{F_i}{\alpha_2}} = e^{\mu\alpha_2}, \tag{3}$$

$$\frac{T_1}{T_2} = e^{\mu\alpha_3}. \tag{4}$$

Cosine Distributed Load

Consider the projectile force to be a cosine-shaped distributed load that varies over angle α_2 and is given by $F_i = a\cos\theta$ (see figure 3), where a is a constant and $0 < \theta < \alpha_2$. Similar to the uniformly distributed load case, there are three contact regions along the crossing yarn. The first and the third contact regions reside over sectors α_1 and α_3 and are governed by the basic friction equation (1); they are represented in equations (5) and (7), respectively. The second contact region over sector α_2 was more complex; it involved several coupled relationships that are given in equation (6). By solving the coupled equations (5) to (7), the ratio of T_1/T_4 can be calculated as shown in equation (7).

$$\frac{T_3}{T_4} = e^{\mu\alpha_1}, \tag{5}$$

$$T_2 = \frac{2\mu a}{1-\mu^2}\sin\left(\frac{\alpha_2}{2}\right) + ce^{\mu\alpha_2}, \tag{6}$$

where

$$c = e^{\mu(\alpha_2/2)}\left(T_3 + \frac{\mu a}{1+\mu^2}\sin\left(\frac{\alpha_2}{2}\right)\right)$$

$$\frac{T_1}{T_2} = e^{\mu\alpha_1}. \tag{7}$$

RESULTS OF UNIFORM AND COSINE DISTRIBUTED LOADS

For the uniformly distributed load case, the variations of angle $\alpha = \alpha_1 + \alpha_2 + \alpha_3$ as a function of the ratio of T_1/T_4, for $\alpha_2 = 0.0°$, 30°, 45°, 60°, and 75°, are depicted in figure 4, where $r = 1$ mm, $F_i = 500$ N, $\mu = 0.4$, and $\omega = 5 \times 10^5$ N/m. As shown in figure 4, both increasing α and increasing α_2 from the basic solution (simple case, $\alpha_2 = 0$) to $\alpha_2 = 75°$ increase the yarn tension ratio T_1/T_4. Figure 4 also reveals that the T_1 tension could reach as high as 3.5 times T_4, which is significant.

Similarly, for the cosine distribution load case, the variations of angle $\alpha = \alpha_1 + \alpha_2 + \alpha_3$ as a function of the ratio of T_1/T_4 , for $\alpha_2 = 0.0°$, 30°, 45°, 60°, and 75°, are depicted in figure 5, where $r = 1$ mm, $F_i = 500$ N, a = 1000 N, $\mu = 0.4$, and $\omega = 5 \times 10^5$ N/m. As shown in figure 5, both increasing α and increasing α_2 from the basic solution (simple case, $\alpha_2 = 0$) to $\alpha_2 = 75°$ increase the yarn tension ratio T_1/T_4. Figure 5 reveals that the T_1 tension could reach as high as 4.5 times T_4, which is also significant. This increase exceeds that of the uniform load case shown in figure 4.

Figures 4 and 5 reflect that the input tension T_1 of a single crossover region is more than double the output tension T_4. Note that for even the smallest angle α_2, pulling a yarn through several crossover regions requires significant force. In addition, the ratio of T_1/T_4 also increases as angle α increases, indicating that the yarn pullout forces in the high crimp content (HCC) yarns are greater than those for low crimp content (LCC) yarns.

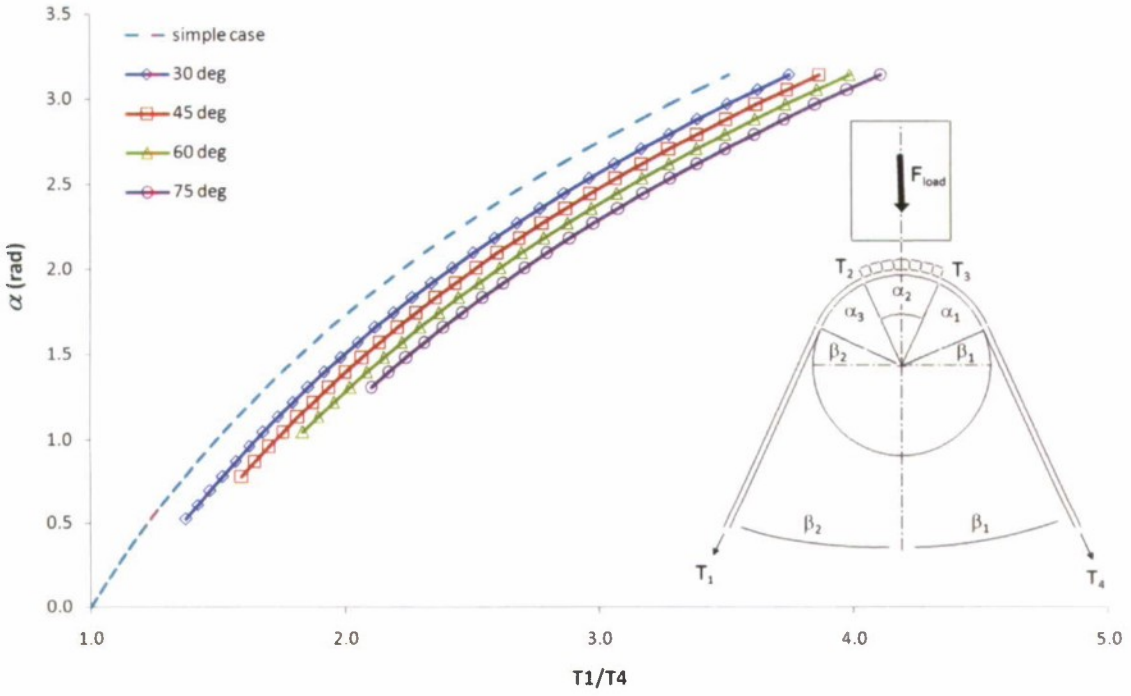

Figure 4. Ratio of T_1/T_4 As a Function of α for α_2 = 0.0°, 30°, 45°, 60°, and 75° for Uniformly Distributed Load

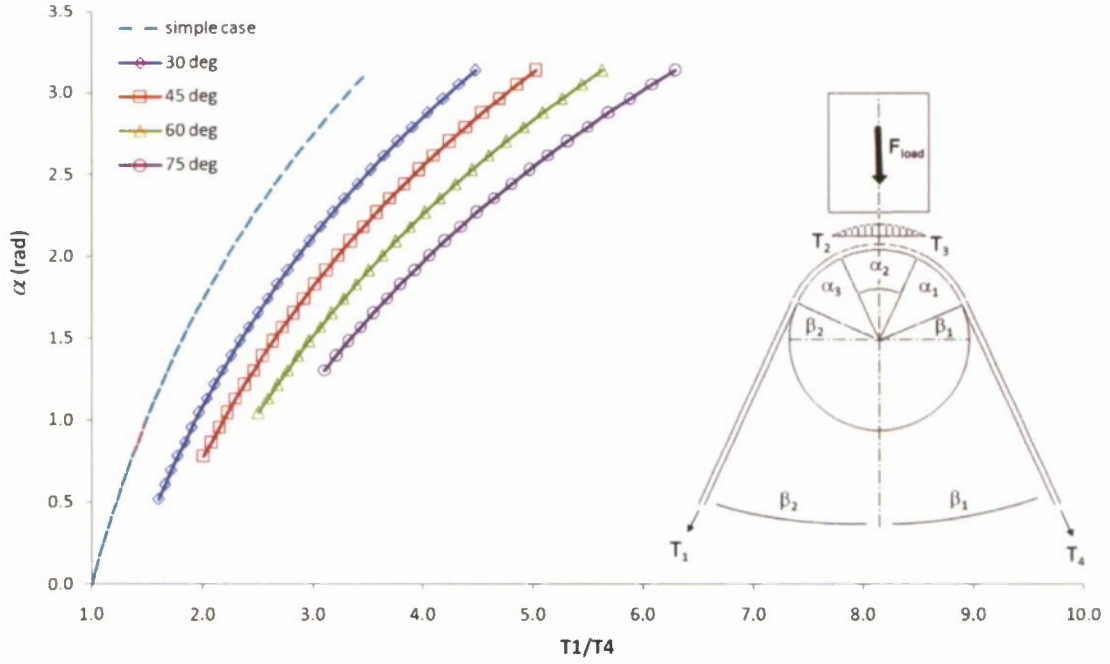

Figure 5. Ratio of T_1/T_4 As a Function of α for α_2 = 0.0°, 30°, 45°, 60°, and 75° for Cosine Distributed Load

PLAIN-WOVEN FABRIC ARCHITECTURE

In addition to unbalanced yarn density ratios, plain-woven fabrics generally have different crimp contents in the warp and weft directions—HCC in the warp yarns and LCC in thc weft yarns. In figure 6, distance h is the distance between centerlines of adjacent crossover regions along the HCC direction; in figure 7, distance t is the distance between centerlines of adjacent crossover regions along the LCC direction. The h and t distances are related to the yarn density ratio (YDR*) of the fabric, which is an important parameter in fabric architecture; h and t distances are therefore important mechanical properties of the fabric.

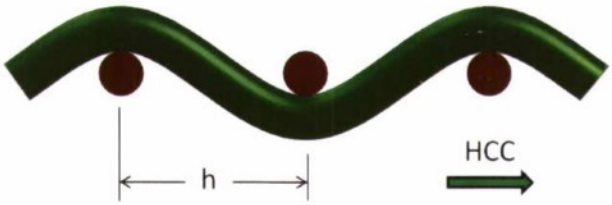

Figure 6. Distance Between the Centerlines of Adjacent Crossover Regions Along the HCC Yarn Direction

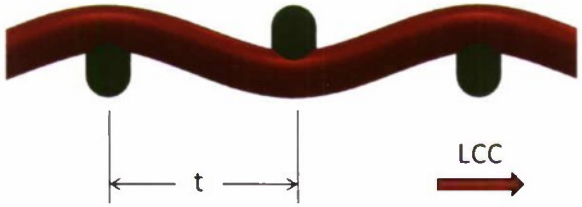

Figure 7. Distance Between Centerlines of Adjacent Crossover Regions Along the LCC Yarn Direction

The crossover region contact angle α in the HCC and LCC yarn directions is geometrically related to centerline distances h and t. Consider first a high crimp content yarn to be a tangent line between two adjacent crossover regions, where the vertical distance of the centerlines of the two adjacent yarns is denoted by x as shown in figure 8.

The relationship between angle α and distances x and h for HCC is

$$\alpha = 2\sin^{-1}\frac{2r}{\sqrt{x^2+h^2}}. \tag{8}$$

* YDR is the ratio of the number of weft yarns per unit length along warp axis to the number of warp yarns per unit length along weft axis.

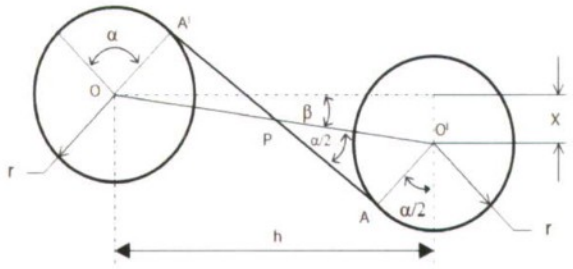

Figure 8. Geometry of Adjacent Crossover Regions Along the HCC Yarn Direction

Consider next an LCC yarn to be a tangent line between two adjacent crossover regions, where the centerline vertical distance of the two adjacent yarns is denoted by y, as shown in figure 9.

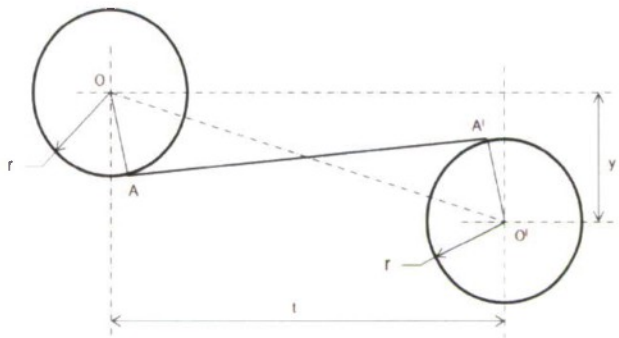

Figure 9. Geometry of Adjacent Crossover Regions Along the LCC Yarn Direction

The relationship between angle α and distances y and t for LCC is

$$\alpha = 2\sin^{-1}\frac{2r}{\sqrt{y^2+t^2}}. \tag{9}$$

Figure 10 depicts the changes in α with respect to h for different values of x (shown as $X1$). As shown, the angle α sharply increases as h is reduced (note that h and $X1$ are in millimeters).

Similarly, figure 11 depicts the changes in α with respect to t for different values of y (shown as $Y1$). As shown, the angle α also sharply increases as t is reduced (note that t and $Y1$ are in millimeters).

Figures 10 and 11 reveal that distances h and t are important parameters in plain-woven fabric architectures. Small changes in h and t significantly affect the yarn crimp contents and, ultimately, the mechanical behavior of the fabric when subjected to loads.

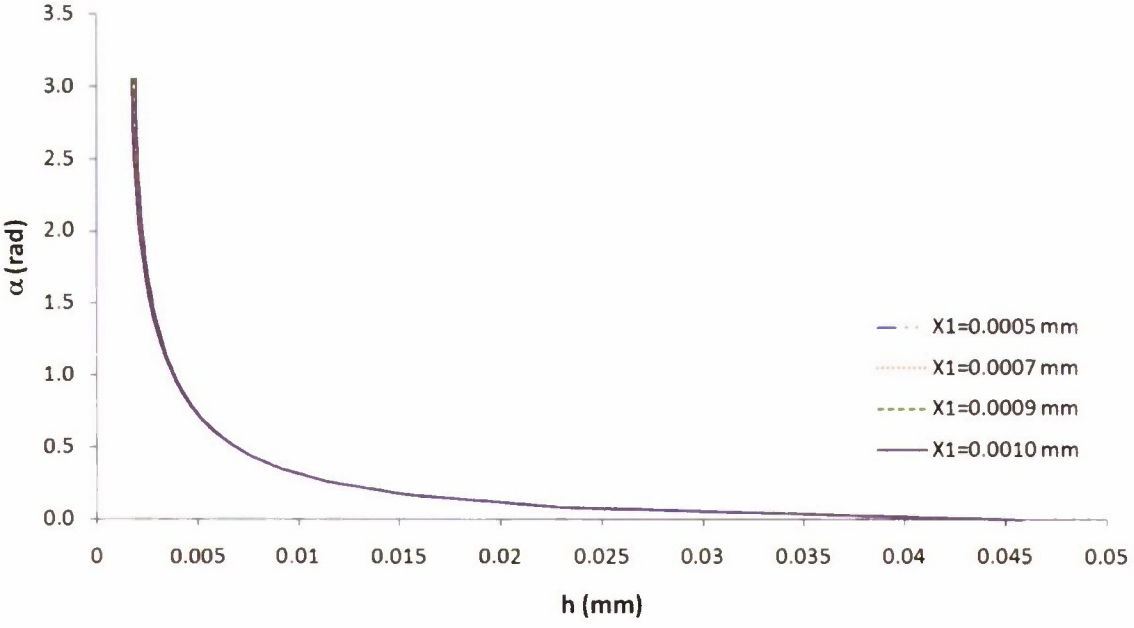

Figure 10. Contact Angle α Varies with h for Different Values of X1

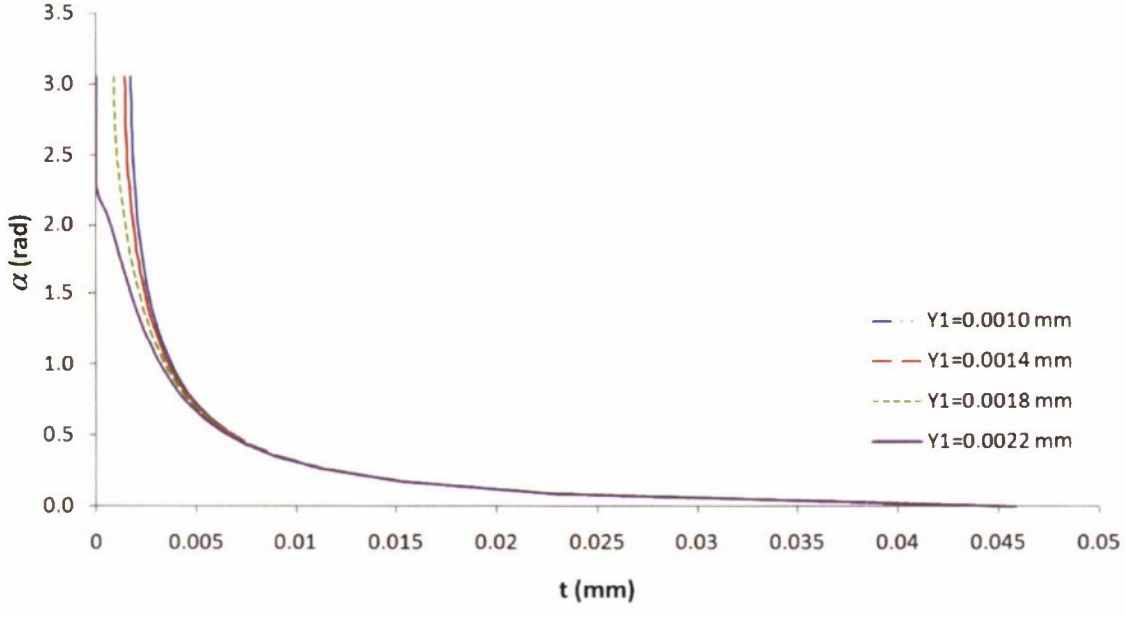

Figure 11. Contact Angle α Varies with t for Different Values of Y1

YARN PULLOUT FORCE OF FABRICS

Two dominant mechanisms of energy absorbability in woven fabrics subject to low-velocity-projectile impacts are yarn migration and yarn stretching. These mechanisms relate to the force required to pull a yarn out from the fabric. If the fabric is made of low-elastic modulus, staple fibers, such as cotton, the pullout force is mainly governed by elastic deformation and elongation of the yarn—the focus of several investigations in which yarn pullout force from plain-woven cotton fabrics was measured.[11,12,13]

On the other hand, if the fibers of a woven fabric are of high-elastic modulus, continuous fibers, such as Kevlar and Armos aramid, then the pullout force is dominated by the crimp interchange and friction over the crossover regions—also the focus of experimental investigations.[14,15] During these two investigations, the fabric was clamped along the bottom edge. Martinez et al.[14] investigated the force required to completely pull out a single Kevlar yarn from a fabric, and Bazhenov[15] investigated the force required to pull out a single Armos aramid yarn from a fabric. Shockey et al.[16] devised an improved pullout test in which the fabric was clamped along its transverse edges.

The analytical formulation of yarn pullout force is of particular interest because it is related to the yarn migration and ballistic protection levels. In the present analysis, the fibers were assumed to be continuous with a high modulus of elasticity and, therefore, the elastic strains in the yarns were neglected. The pullout test is, therefore, largely governed by the frictional phenomenon at the crossover regions.

YARN PULLOUT FORCE WITHOUT PROJECTILE LOAD

Consider a swatch of plain-woven fabric constructed of n number of HCC yarns in the warp direction and n number of LCC yarns in the weft direction; that is, there are n x n number of crossover regions. Thus, an HCC yarn has n number of crossover regions, as shown in figure 12. Based on the weaving architecture and the distance between two adjacent yarns, the contact angle is α at every crossover region. In this case, it is assumed that there is no external load present (that is, there is no force due to projectile impact).

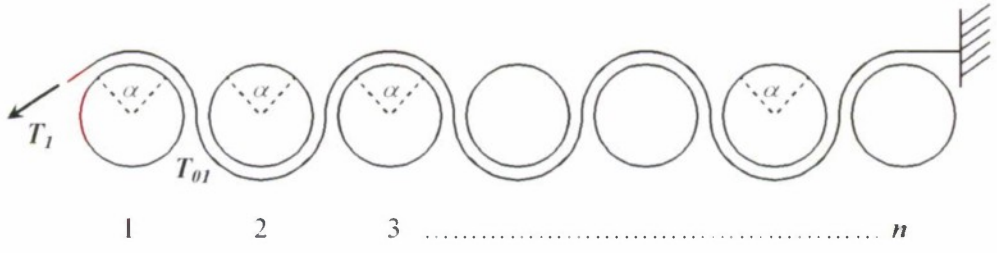

Figure 12. n Number of Crossover Regions for an HCC Yarn

Denoting the pullout tension as T_1 and the yarn tension on the n^{th} (last) crossover region as T_n, the ratio of the first and the last tensions is

$$\frac{T_1}{T_n} = e^{\mu(\alpha+\alpha+\cdots\alpha)} = e^{\mu n\alpha}. \tag{10}$$

Figure 13(a) shows the ratio $Q = T_1/T_n$ as a function of the number of crossover regions n for different contact angles α, and figure 13(b) shows the ratio $Q = T_1/T_n$ as a function of the different values of the coefficient of friction μ. Note that μ varies between 0.1 and 0.4.

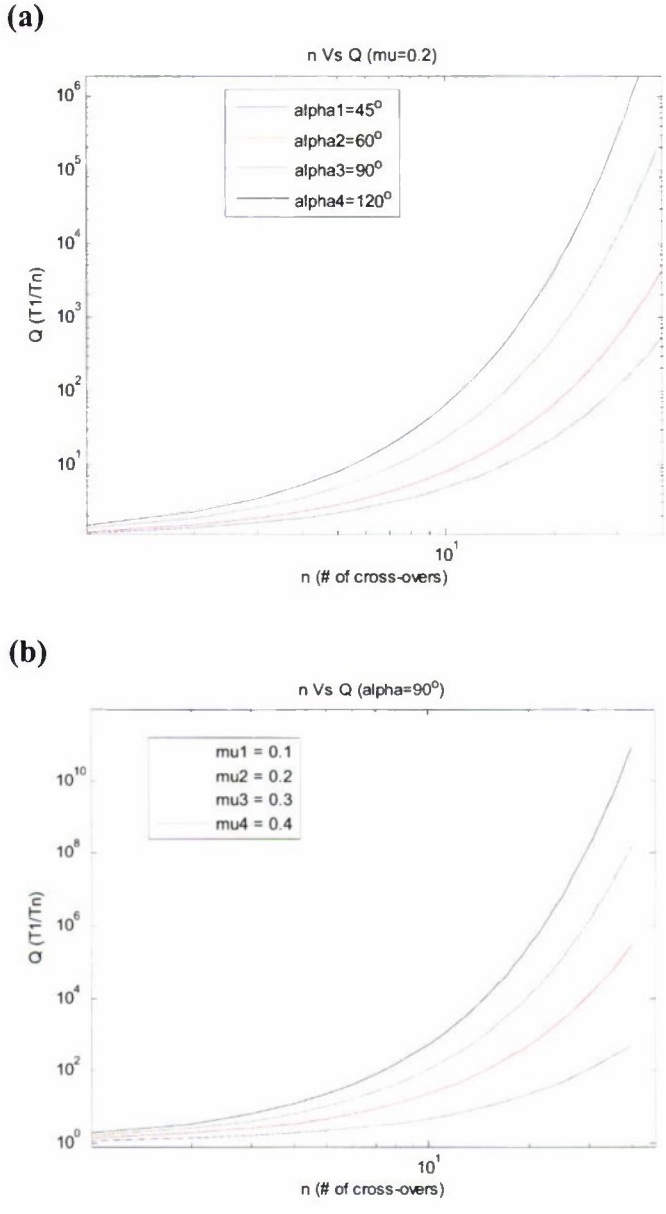

Figure 13. (a) $Q = T_1/T_n$ As a Function of n for Different Values of α and (b) $Q = T_1/T_n$ As a Function of n for Different Coefficient of Friction Values

YARN PULLOUT FORCE WITH PROJECTILE LOAD

Load Estimation

During a low-velocity-projectile impact event, the projectile contacts a plain-woven fabric swatch of size L x L (for example, 40 x 40 mm^2) and the fabric initially deflects where its boundaries are clamped. The global fabric deflection δ is shown in figure 14(b).

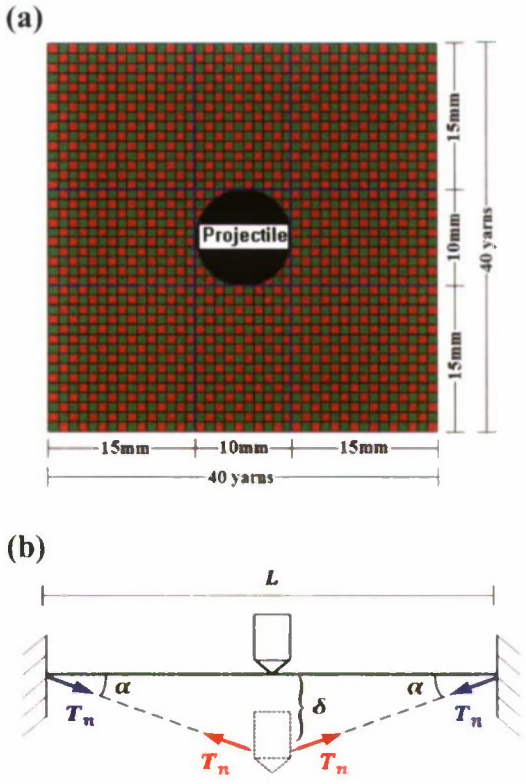

Figure 14. (a) Top View of the Fabric with Its Dimensions and Location of the Projectile, (b) Schematic Cross-Sectional View of the Fabric Showing Global Deflection δ and Tension T_n

Thus, the tension in the i^{th} yarn (T_{ni}) is computed by

$$T_{ni} = F_i/(2\sin\alpha) = F_i/(2(2\delta/L)) = F_iL/4\delta,$$

where F_i is the projectile impact force on the yarn. In an extreme case, if the fabric stops the projectile, and based on the work-energy relationship, then the tension in the i^{th} yarn is $F_i\delta = 1/2mV^2$. To estimate the range of projectile force F_i and yarn tension T_{ni}, one must make the following assumptions:

1. The projectile velocity is 300 m/sec.

2. The projectile weight is 10 grams (0.01 kg).

3. The projectile is shaped as a right circular cylinder (RCC) with a cross-sectional diameter of 10 mm.

4. The coefficient of friction at the yarn-yarn contact interfaces is 0.1 to 0.4.

5. The fabric is square, having sides L x L, where L is 1 m.

6. The fabric global deflection δ due to projectile contact is approximatcly 10% of the fabric length.

Based on these assumptions, the average projectile force on each yarn F_i is 70 N. Because the assumptions may not reflect an actual impact force, a wider range of this force, namely 40 N to 100 N was considered. For this range of impact force, tension in the yarn varies betwcen 175 N to 250 N. To cover a wider range of yarn tension, the range of T_i = 100 to 500 N is used.

Projectile Contact Cases

Case 1: Projectile Contacts Every Other Crossover Region. For a crimp-imbalanced plain-woven fabric, the superior section of the yarns at crossover regions will not lie on the same plane; therefore, when a projectile contacts the fabric, contact is established at every other crossover region, as shown in figure 15. The equation for the yarn tension, therefore, varies from one crossover region to the next. For example, consider only 10 crossover regions, where five (every other) crossover regions establish contact with the projectile. Denoting the tension on the outside of the 10^{th} crossovcr region as T_{10}, one can calculate the pullout tension T_1 on the first crossover region, as shown in equations (11).

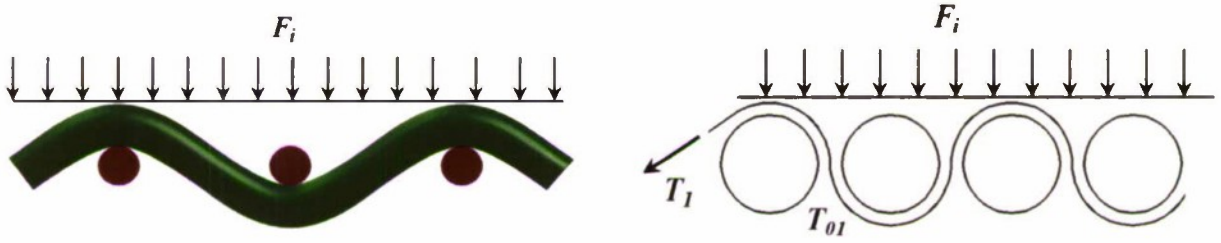

Figure 15. Pattern Showing RCC Projectile Contact at Every Other Crossover Region for a Crimp-Imbalanced Architecture

The equation for each of the ten considered crossover regions is given in equations (11):

$$\text{Crossover Region 1:} \quad \frac{T_1 + \frac{F_i}{\alpha}}{T_2 + \frac{F_i}{\alpha}} = e^{\mu\alpha},$$

$$\text{Crossover Region 2:} \quad \frac{T_2}{T_3} = e^{\mu\alpha},$$

$$\text{Crossover Region 3:} \quad \frac{T_3 + \frac{F_i}{\alpha}}{T_4 + \frac{F_i}{\alpha}} = e^{\mu\alpha},$$

$$\text{Crossover Region 4:} \quad \frac{T_4}{T_5} = e^{\mu\alpha},$$

$$\text{Crossover Region 5:} \quad \frac{T_5 + \frac{F_i}{\alpha}}{T_6 + \frac{F_i}{\alpha}} = e^{\mu\alpha}, \tag{11}$$

$$\text{Crossover Region 6:} \quad \frac{T_6}{T_7} = e^{\mu\alpha},$$

$$\text{Crossover Region 7:} \quad \frac{T_7 + \frac{F_i}{\alpha}}{T_8 + \frac{F_i}{\alpha}} = e^{\mu\alpha},$$

$$\text{Crossover Region 8:} \quad \frac{T_8}{T_9} = e^{\mu\alpha},$$

$$\text{Crossover Region 9:} \quad \frac{T_9 + \frac{F_i}{\alpha}}{T_{10} + \frac{F_i}{\alpha}} = e^{\mu\alpha}.$$

For this case, the results are shown in figure 16, where the pullout force T_1 is depicted as a function of α, for different values of T_{10} (ranging from 100 to 500 N) and different contact forces of F_i (F_i is 40 N in figure 16(a) and is 100 N in figure 16(b)). Note that increasing α, which increases the crimp contents in the HCC yarns, exponentially increases the pullout force.

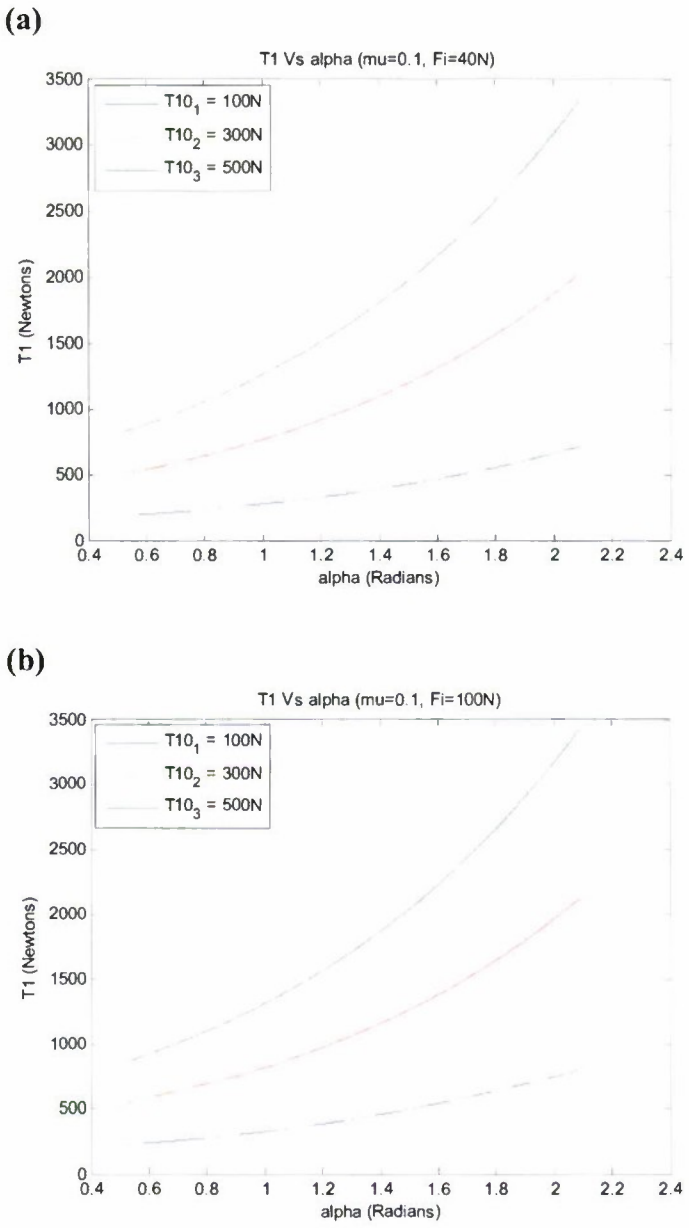

Figure 16. Yarn Pullout Force T_1 As a Function of α for Different Values of T_{10} and F_i When an RCC Projectile Contacts Every Other Crossover Region: (a) F_i = 40 N and (b) F_i = 100 N

Case 2: Projectile Contacts All Crossover Regions. In this case, the fabric architecture is crimp-balanced and the projectile contact force is applied to all crossover regions, as shown in figure 17. Thus, the equation of tension at each crossover region is given by equation (12); the relationship between the first and the last tension, therefore, is given in equation (12).

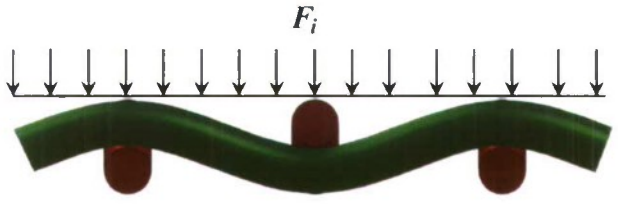

Figure 17. Pattern Showing RCC Projectile Contact at All Crossover Regions for a Crimp-Balanced Architecture

$$\frac{T_1 + \dfrac{F_i}{\alpha}}{T_{n+1} + \dfrac{F_i}{\alpha}} = e^{\mu n \alpha}. \tag{12}$$

For this case, 10 crossover regions were considered. Figure 18 depicts the results of pullout force T_1 as a function of α, for different values of T_{10} (ranging from 100 to 500 N) and different values of contact forces F_i, (F_i is 40 N in figure 18(a) and 100 N in figure 18(b)). Note that, as in the previous case, increasing α, which increases the crimp content in the HCC yarns, exponentially increases the pullout force.

(a)

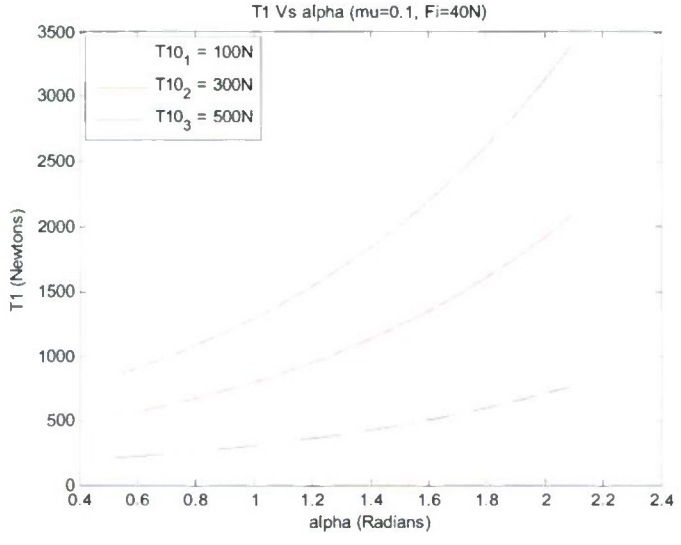

Figure 18. Yarn Pullout Force T_1 As a Function of α for Different Values of T_{10} and F_i When an RCC Projectile Contacts Every Crossover Region: (a) F_i = 40 N and (b) F_i = 100 N

(b)

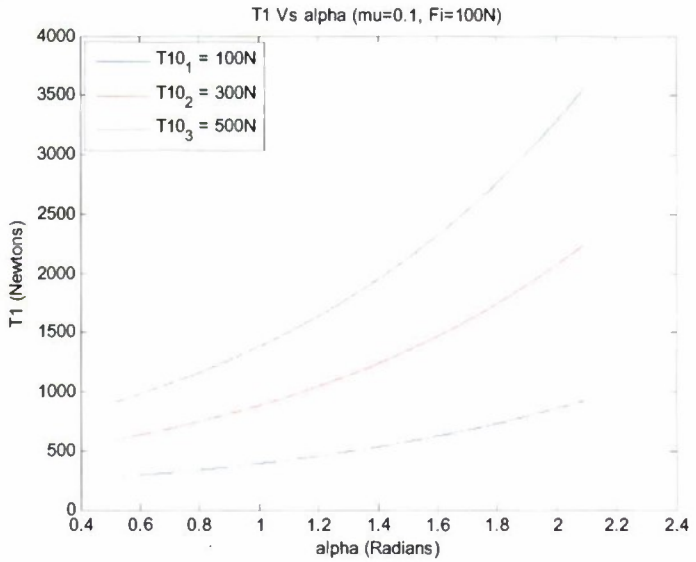

Figure 18. Yarn Pullout Force T_1 As a Function of α for Different Values of T_{10} and F_i When an RCC Projectile Contacts Every Crossover Region: (a) F_i = 40 N and (b) F_i = 100 N (Cont'd)

YARN MIGRATION FORCES

Referring to figure 19, when a projectile contacts a woven fabric during a low-velocity impact, the projectile initially deflects the fabric plane and induces migration of the primary yarns away from the impact zone. These primary yarn migrations shown in figure (19c) lead to the formation of openings between adjacent yarns, which permit the projectile to penetrate the fabric without yarn failure. (Recall the invoked assumption that yarn failures were not permitted in the current analysis.) Note that, compared to HCC yarns, the LCC yarns have less crimp content.

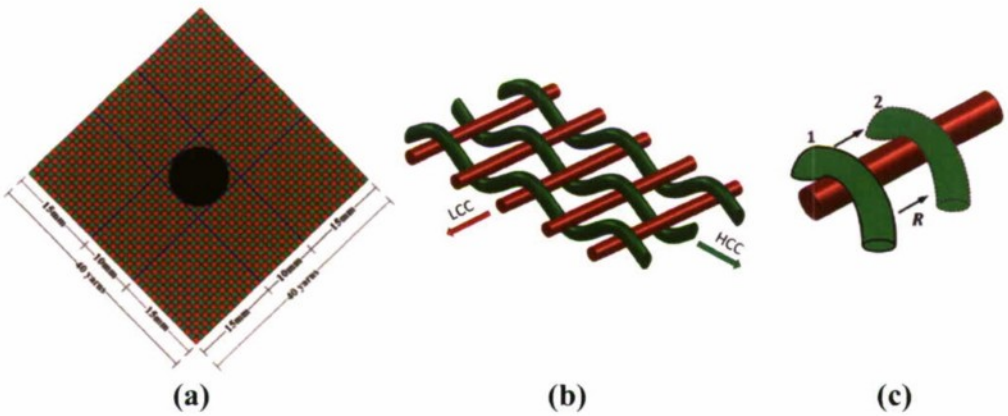

Figure 19. (a) Plain-Woven Fabric, (b) HCC Yarns Aligned in the Warp Direction and LCC Yarns Aligned in the Weft Direction, and (c) Migration Phenomenon

Primary yarn migrations occur when a primary yarn slides in the direction perpendicular to its axis over a erossing yarn as shown in figure 19(c). This migration phenomenon results from the limited frictional force (that is, limited slip resistanee) developed at the crossover regions. Let the migration force on the yarns in the HCC or the LCC direction be denoted by R. Two issues are addressed in the following seetions: (1) the meehanism to separate the yarns and (2) the magnitude of foree required to generate an opening sufficiently sized to permit a projectile to penetrate through.

MIGRATION FORCE WITHOUT PROJECTILE LOAD

The free-body diagram of a single erossover region is shown in figure 20. Using statie equilibrium, the migration foree R_1 (in the direetion perpendieular to the page) ean be derived as $R_1 = \mu(T_1 + T_2)\sin\alpha/2$. Consider a yarn that spans n crossover regions: the general formula for the total migration force R for the n crossover region is given by

$$R = \sum_{i=1}^{n-1} R_i = \mu \sin\left(\frac{\alpha}{2}\right)\left[2\sum_{i=1}^{n} T_i - (T_1 + T_{n+1})\right].$$

Substituting $T_i = (T_{i+1})e^{\mu\alpha_i}$, and repeating this proeess, one ean arrive at:

$$R = \mu \sin\left(\frac{\alpha}{2}\right)\left[T_n \times 2 \times \frac{e^{\mu\alpha(11)} - 1}{e^{\mu\alpha} - 1} - T_n\left(1 + e^{\mu\alpha(n)}\right)\right]. \tag{13}$$

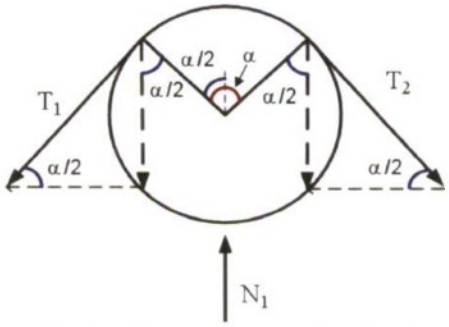

Figure 20. Free-Body Diagram of a Single Crossover Region

Consider now, for example, a yarn spanning 10 erossover regions. The equation for the migration foree is then given by equation (13). To make the foree nondimensional, T_{10} is faetored out and the results are given in terms of $P = R/T_n$. Figure 21 depiets the variation of P with respect to the number of erossover regions n for various values of α and eoefficients of friction μ. As shown in figure 21, increasing α (that is, higher crimp eontent) exponentially inereases the migration foree—similar to the pullout foree deseribed in the previous section.

$$P = R/T_{10} = \mu \sin\left(\frac{\alpha}{2}\right)\left[2 \times \frac{e^{\mu\alpha(11)} - 1}{e^{\mu\alpha} - 1} - \left(1 + e^{\mu\alpha(10)}\right)\right]. \tag{14}$$

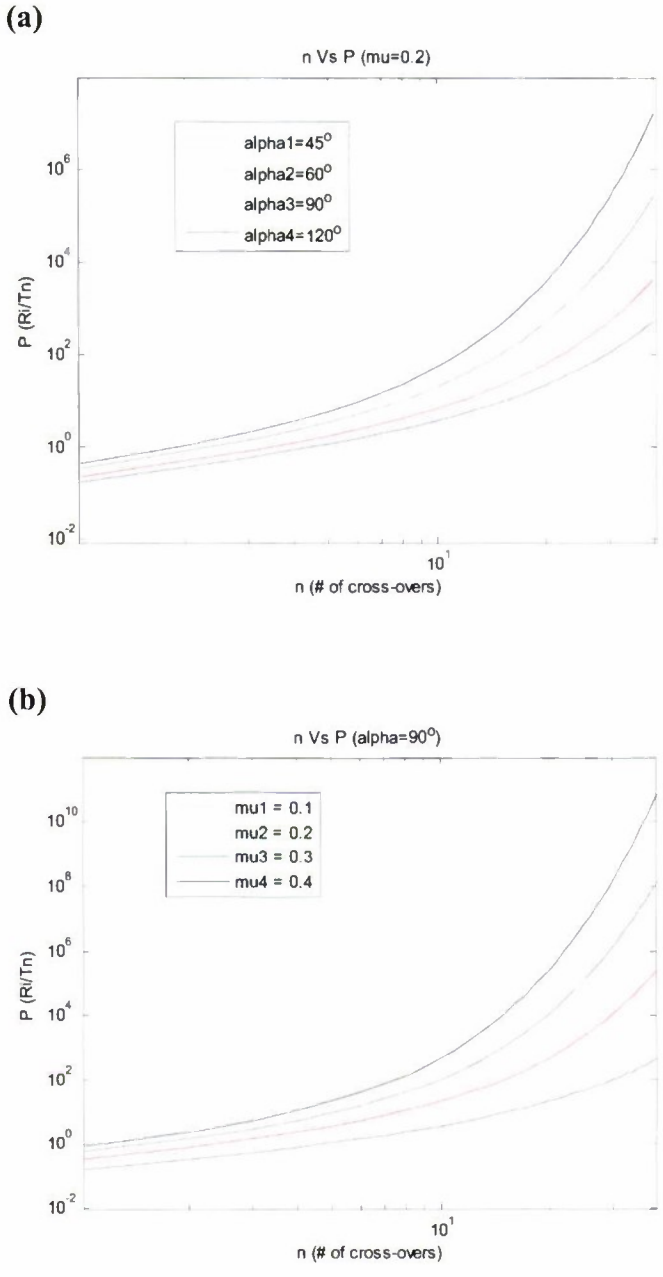

Figure 21. (a) Migration Force Ratio P Versus Number of Crossover Regions (for μ = 0.2, α = 45°, 60°, 90°, 120°) and (b) Migration Force Ratio P Versus Number of Crossover Regions (for μ = 0.1, 0.2, 0.3, 0.4)

MIGRATION FORCE WITH PROJECTILE LOAD

As with the pullout force discussion in the previous section, two projectile contact cases are described in this section: one in which the projectile contacts every other crossover region (that is, crimp-imbalanced architecture) and one in which the projectile contacts all crossover regions (that is, crimp-balanced architecture).

Projectile Contact Cases

Case 1: Projectile Contacts Every Other Crossover Region. The free-body diagram of a single crossover region in a crimp-imbalanced architecture is shown in figure 22.

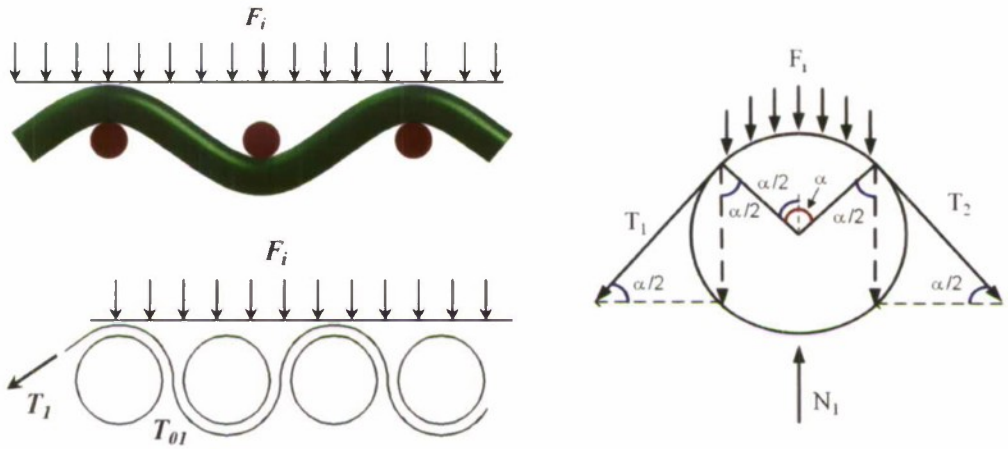

Figure 22. Schematic and Free-Body Diagrams of Crossover Regions in a Crimp-Imbalanced Architecture

Using the equilibrium of the crossover region, the migration force R_1 can be derived as:

$$N_1 = T_1 \sin\left(\frac{\alpha}{2}\right) + T_2 \sin\left(\frac{\alpha}{2}\right) + F_i,$$

$$R_1 = \mu N_1,$$

$$R_1 = \mu(T_1 + T_2)\sin\left(\frac{\alpha}{2}\right) + \mu F_i.$$

For the noncontact crossover region, the migration force is similar to that described for the pullout force:

$$R_2 = \mu(T_2 + T_3)\sin\left(\frac{\alpha}{2}\right).$$

The equations for R_1 and R_2 can be expanded for n crossover regions. For example, consider ten crossover regions: the tension in the last crossover region is T_{10}. The equations for crossover regions 3 through 9 are given below:

Crossover Region 1: $$R_1 = \mu(T_1 + T_2)\sin\left(\frac{\alpha}{2}\right) + \mu F_i.$$

Crossover Region 2: $$R_2 = \mu(T_2 + T_3)\sin\left(\frac{\alpha}{2}\right).$$

Crossover Region 3: $$R_3 = \mu(T_3 + T_4)\sin\left(\frac{\alpha}{2}\right) + \mu F_i,$$

Crossover Region 4: $$R_4 = \mu(T_4 + T_5)\sin\left(\frac{\alpha}{2}\right) + \mu F_i,$$

$\vdots$ $\vdots$

Crossover Region 9: $$R_9 = \mu(T_9 + T_{10})\sin\left(\frac{\alpha}{2}\right) + \mu F_i.$$

Finally, the total migration force for the nine crossover regions is given by equation (15):

$$R = \mu\sin\left(\frac{\alpha}{2}\right)\left[T_{10} \times 2 \times \frac{e^{\mu\alpha(11)} - 1}{e^{\mu\alpha} - 1} - T_{10}\left(1 + e^{\mu\alpha(10)}\right)\right] + 4\mu F_i. \tag{15}$$

For n number of crossover regions,

$$R = \mu\sin\left(\frac{\alpha}{2}\right) \times T_n\left[2 \times \frac{e^{\mu\alpha(n+1)} - 1}{e^{\mu\alpha} - 1} - \left(1 + e^{\mu\alpha(n)}\right)\right] + \frac{(n-1)}{2}\mu F_i$$

The variation of the migration force R as a function of α, for different values of T_{10} and different values of external force F_i, is depicted in figure 23.

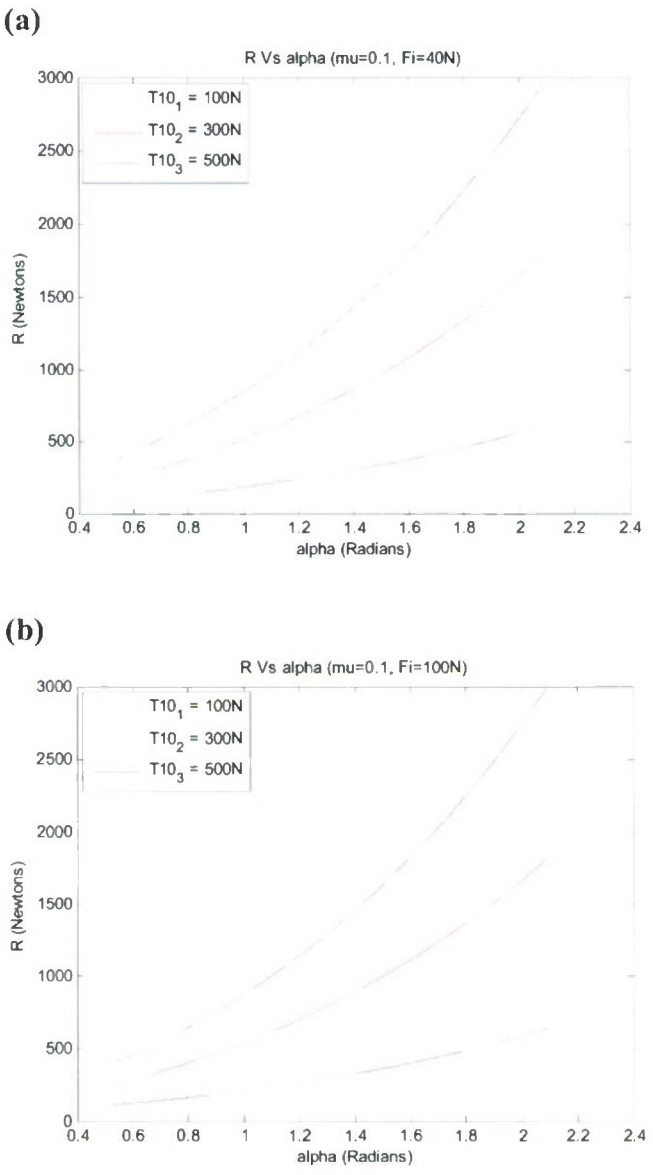

Figure 23. Migration Force R for Different Values of T_{10} and Different Values of External Force F_i (for Every Other Crossover Region): (a) F_i = 40 N and (b) F_i = 100 N

Case 2: Projectile Contacts All Crossover Regions. As shown in figure 24, the projectile contacts all crossover regions in a crimp-balanced architecture. In this case, the migration force for each crossover region is given by the following sequence of equations:

$$R_1 = \mu(T_1 + T_2)\sin\left(\frac{\alpha}{2}\right) + \mu F_i,$$

$$R_2 = \mu(T_2 + T_3)\sin\left(\frac{\alpha}{2}\right) + \mu F_i,$$

$$R_i = \mu(T_i + T_{i+1})\sin\left(\frac{\alpha}{2}\right) + \mu F_i = \mu\left(T_{i+1}e^{\mu\alpha} + T_{i+1}\right)\sin\left(\frac{\alpha}{2}\right) + F_i.$$

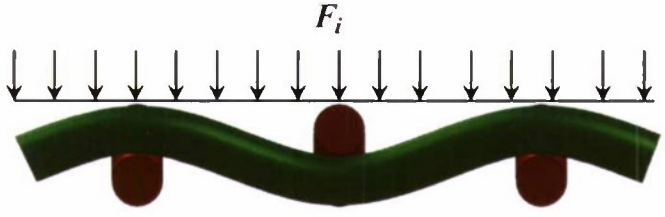

Figure 24. Pattern Showing Projectile Contacting All Crossover Regions in a Crimp-Balanced Architecture

In general, for n crossover regions, the migration force is

$$R = \sum_{i=1}^{n-1} R_i = \mu\sin\left(\frac{\alpha}{2}\right)\left[2\sum_{i=1}^{n} T_i - (T_1 + T_{n+1})\right] + n\mu F_i. \tag{16}$$

As an example, consider nine crossover regions. The ninth migration force is

$$R_9 = \mu(T_9 + T_{10})\sin\left(\frac{\alpha}{2}\right) + \mu F_i.$$

Summing all migration forces for the nine crossover regions and using the basic relationship between two tensions $T_1 = T_2 e^{\mu\alpha}$, the total migration force is given by equation (17). Note that this equation is a different form of equation (16).

$$R = \sum_{i=1}^{n} R_i = \mu\sin\left(\frac{\alpha}{2}\right)\left[T_{10}\left(e^{9\mu\alpha} + 2\left(e^{8\mu\alpha} + e^{7\mu\alpha} + e^{6\mu\alpha} + e^{5\mu\alpha} + e^{4\mu\alpha} + e^{3\mu\alpha} + e^{2\mu\alpha} + e^{\mu\alpha}\right) + 1\right)\right] + 9\mu F_i.$$

(17)

Figure 25 depicts the variation of migration force R with respect to α for different values of T_{10} and F_i. The coefficient of friction μ is assumed to be 0.1. As shown in figure 25, increasing α (which increases the crimp content of the HCC yarns), exponentially increases the migration force, a response similar to that observed for the pullout force.

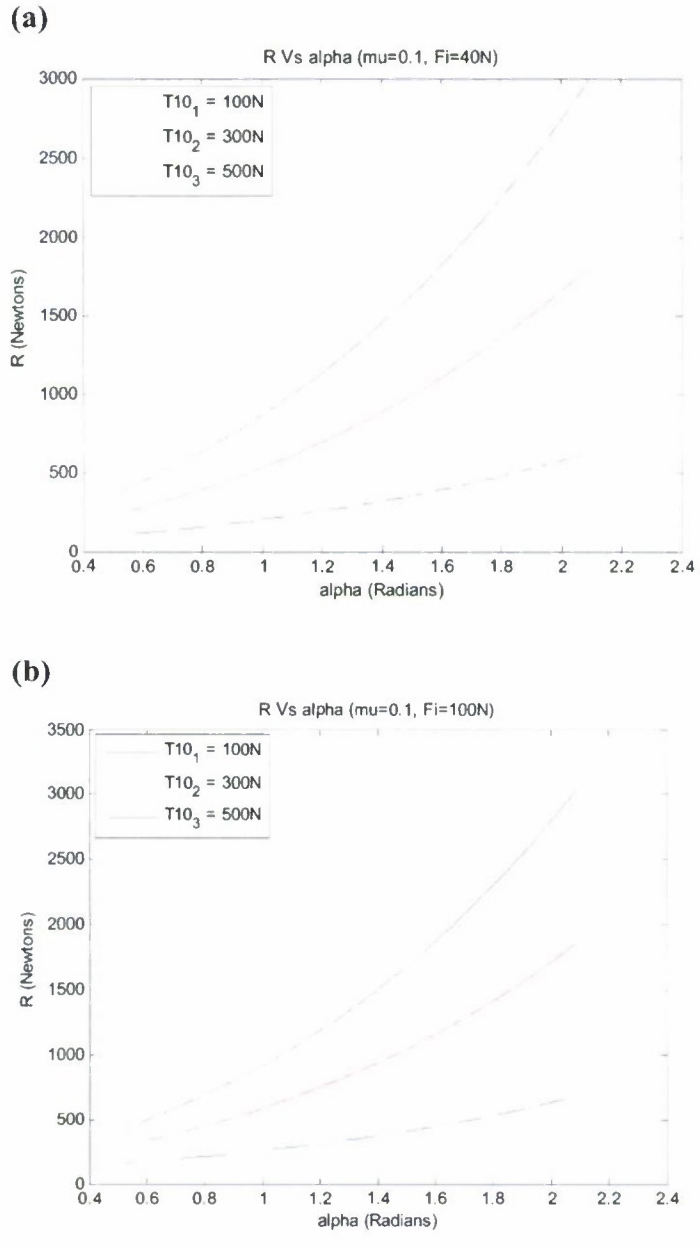

Figure 25. Migration Force R for Different Values of T_{10} and Different Values of External Force F_i (for All Crossover Regions): (a) F_i= 40 N and (b) F_i= 100 N

ENERGY ABSORPTION AND RESIDUAL VELOCITY

This section explores the relationship between the energy absorbed by yarn pullout, yarn migration, and the residual velocity of the projectile. It was assumed that the projectile created an opening in the fabric of diameter D. The work done by yarn pullout and yarn migration for 2 x 2, 4 x 4, and 8 x 8 yarn fabrics swatches was derived. The work done was equated to the change in kinetic energy of the projectile, and finally, the residual velocity of the projectile was determined.

YARN PULLOUT AND MIGRATION FOR 2 X 2, 4 X 4, AND 8 X 8 FAMILIES OF YARNS

When a projectile contacts a woven fabric, relative motions of the primary yarns occur that lead to crimp interchange, yarn stretch, yarn pullout, fabric shearing, and yarn migration. For projectiles with conical leading edges, the projectile's geometry is even more capable of pushing aside yarns in its path, which eventually leads to the formations of openings within the fabric sufficiently sized to enable penetration to occur without yarn fractures. To create a sufficiently sized opening, yarns of each family migrate along their relative orthogonal directions

In this study, pullout forces are denoted by T_i and migration forces are denoted by R_i, as shown in figure 26 for a 2 x 2 representation of plain-woven yarns. Note that, along the HCC yarn direction, the contact angle α is denoted by α_x or α_{HCC}; similarly, along the LCC yarn direction, the contact angle α is denoted by α_y or α_{LCC}. Pullout tensions T associated with the HCC and LCC directions are denoted by $T_x = T^{HCC}$ and $T_y = T^{LCC}$, respectively. Likewise, the migration forces R associated with the HCC and LCC directions are denoted by $R_x = R^{HCC}$ and $R_y = R^{LCC}$, respectively. Note that T_{ix} or T_{iy} can be determined by using the pullout equations (11) or (12); therefore, the equations for T_{ix} or T_{iy} are not repeated here.

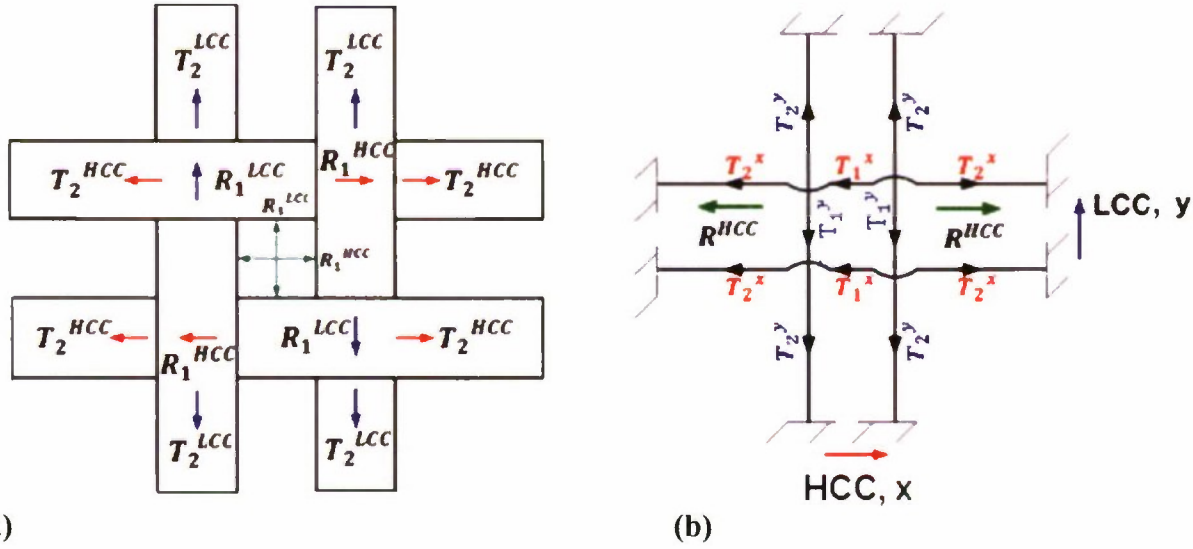

Figure 26. (a) 2 x 2 Yarn Plain-Woven Fabric Representation and (b) Pullout (T_i) and Migration (R_i) Force Descriptions

For the 2 x 2 plain-woven yarn case, the migration force in the x-direction (HCC direction) can be derived as

$$R_x = R^{HCC} = 4R_{1x} = 4\mu\left(T_{2x}e^{\mu\alpha_x} + T_{2x}\right)\sin\left(\frac{\alpha_x}{2}\right),$$

$$R_x = 4\mu\left(1 + e^{\mu\alpha_x}\right)T_{2x}\sin\left(\frac{\alpha_x}{2}\right). \tag{18}$$

Similarly, the migration force in the y-direction (LCC direction) can be derived as

$$R_y = R^{LCC} = 4R_{1y} = 4\mu\left(T_{2y}e^{\mu\alpha_y} + T_{2y}\right)\sin\left(\frac{\alpha_y}{2}\right),$$

$$R_y = 4\mu\left(1 + e^{\mu\alpha_y}\right)T_{2y}\sin\left(\frac{\alpha_y}{2}\right). \tag{19}$$

Consider a 4 x 4 plain-woven fabric as depicted in figure 27.

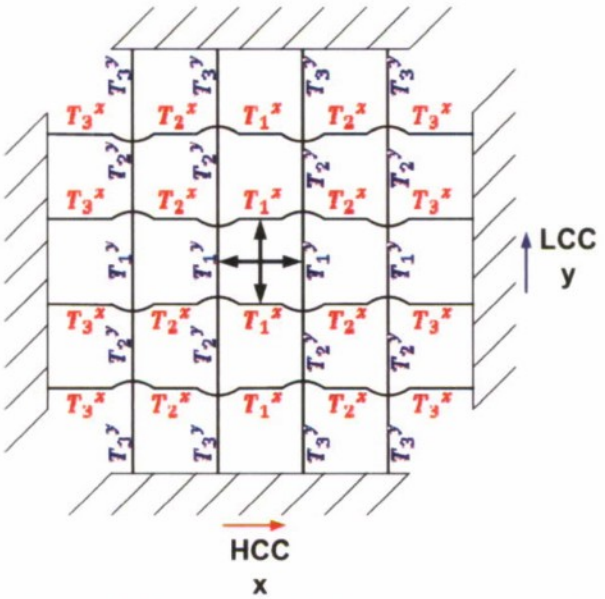

Figure 27. Pullout (T_i) and Migration (R_i) Forces in a 4 x 4 Plain-Woven Fabric

For the 4 x 4 plain-woven fabric case, the migration force in the x-direction (HCC direction) can be derived as

$$R_x = R^{HCC} = 8R_{1x} + 8R_{2x},$$

$$R_x = 8\mu\left(T_{1x} + 2T_{2x} + T_{3x}\right)\sin\left(\frac{\alpha_x}{2}\right). \tag{20}$$

Similarly, the migration force in the y-direction R_y can be derived as

$$R_y = R^{HCC} = 8R_{1y} + 8R_{2y},$$

$$R_y = 8\mu\left(T_{1y} + 2T_{2y} + T_{3y}\right)\sin\left(\frac{\alpha_y}{2}\right). \tag{21}$$

Consider the 8 x 8 plain-woven case shown in figure 28.

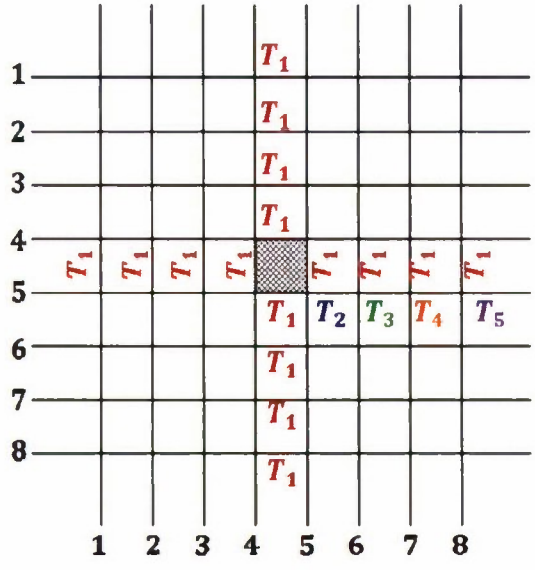

Figure 28. 8 x 8 Plain-Woven Fabric

For the 8 x 8 plain-woven fabric case, the migration force in the x-direction (HCC direction) can be derived as

$$R_x = R^{HCC} = 16R_{1x} + 16R_{2x} + 16R_{3x} + 16R_{4x},$$

$$R_x = 16\mu\sin\left(\frac{\alpha_x}{2}\right)\left(T_{1x} + 2T_{2x} + 2T_{3x} + 2T_{4x} + T_{5x}\right). \tag{22}$$

Similarly, the migration force in the y-direction R_y can be derived as

$$R_y = R^{HCC} = 16R_{1y} + 16R_{2y} + 16R_{3y} + 16R_{4y},$$

$$R_y = 16\mu\sin\left(\frac{\alpha_y}{2}\right)\left(T_{1y} + 2T_{2y} + 2T_{3y} + 2T_{4y} + T_{5y}\right). \tag{23}$$

Note that, if the fabric is also subjected to projectile impact force F_i, then the term $n\mu F_i$ should be added to equations (18) to (23). For all the plain-woven fabric cases (2 x 2, 4 x 4, and 8 x 8),

the pullout forces T_{ix} or T_{iy} ean be determined by using equations (11) or (12). Note also that the differenee between R_x and R_y is the contact angles of α_x or α_{HCC} and α_y or α_{LCC}.

To quantify the values of migration force R, eonsider the 8 x 8 plain-woven case. The results of R_x and R_y as a function of α for different T_5 (the last pullout foree) and for different F_i are shown in figures 29 and 30.

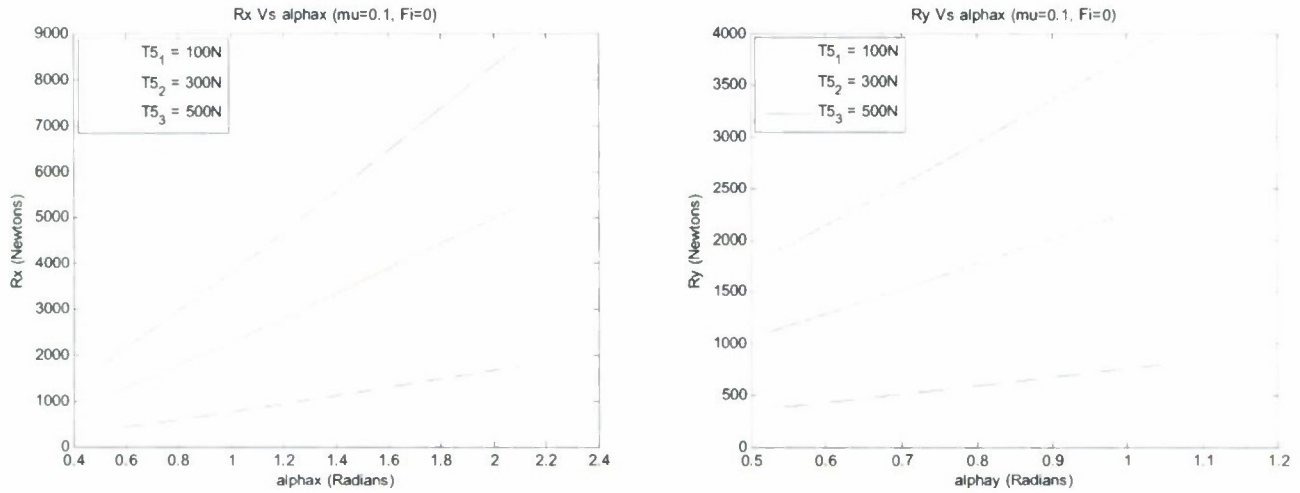

(a) (b)

Figure 29. (a) R_x Migration Forces As a Function of α for Different Values of T_5 and $F_i = 0$ and (b) R_y Forces As a Function of α for Different Values of T_5 and $F_i = 0$

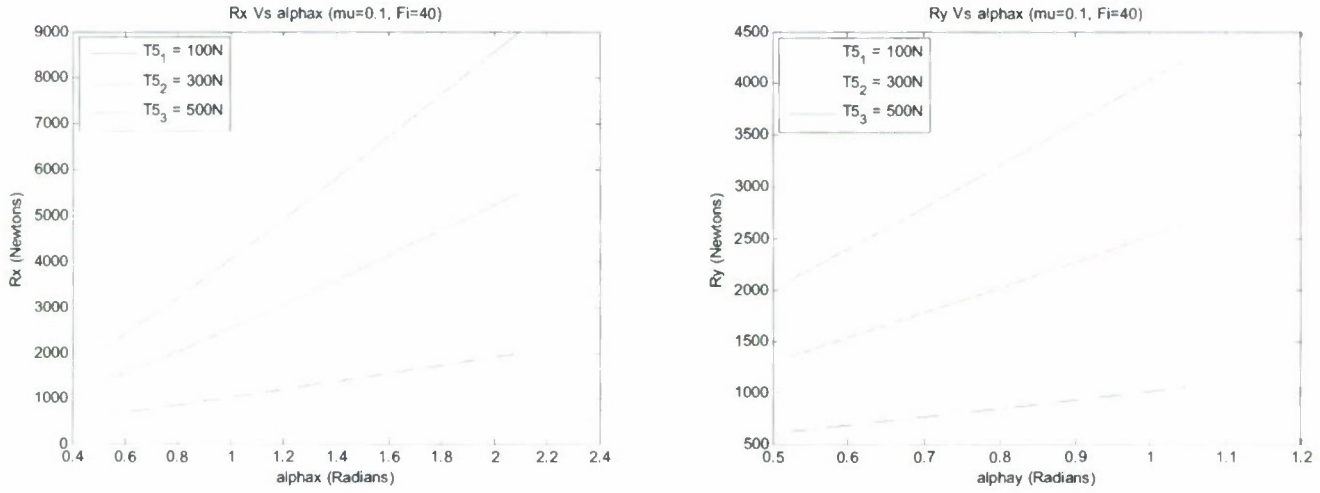

(a) (b)

Figure 30. (a) R_x Migration Forces As a Function of α for Different Values of T_5 and $F_i = 40$ and (b) R_y Forces As a Function of α for Different Values of T_5 and $F_i = 40$

GENERAL FORMULATION FOR PLAIN-WOVEN FABRIC OF *N* X *N* YARNS

The equation for the migration force for *n* x *n* yarns in the x-direction R_x is

$$R_x = R^{HCC} = 2n\left(R_{1x} + \cdots + 16R_{nx}\right),$$

$$R_x = 2n\mu\sin\left(\frac{\alpha_x}{2}\right)\left[2\sum_{i=1}^{n+1} T_{ix} - \left(T_{ix} + T_{(n+1)x}\right)\right] + n\mu Fi. \tag{24}$$

The equation for the migration force for *n* x *n* yarns in the y-direction R_y is

$$R_y = R^{LCC} = 2n\left(R_{1y} + \cdots 16R_{ny}\right),$$

$$R_y = 2n\mu\sin\left(\frac{\alpha_y}{2}\right)\left[2\sum_{i=1}^{n+1} T_{iy} - \left(T_{1y} + T_{(n+1)y}\right)\right] + n\mu F_i. \tag{25}$$

Any successive T_i values in the equations (24) and (25) are derived from equations (26), as developed in previous sections.

In x-direction,

$$\frac{T_n + \dfrac{F_i}{\alpha_x}}{T_{n+1} + \dfrac{F_i}{\alpha_x}} = e^{\mu\alpha_x},$$

and in the y-direction,

$$\frac{T_n + \dfrac{F_i}{\alpha_y}}{T_{n+1} + \dfrac{F_i}{\alpha_y}} = e^{\mu\alpha_y}. \tag{26}$$

The relationship between the first and the last tension for the n^{th} crossover region is given by

$$\frac{T_1 + \dfrac{F_i}{\alpha}}{T_{n+1} + \dfrac{F_i}{\alpha}} = e^{\mu n\alpha}, \tag{27}$$

where the angle α can be replaced by α_x or α_y.

ENERGY AND RESIDUAL VELOCITY

When a projectile with a conically shaped leading edge contacts a fabric at low velocity, the plane of the fabric deflects causing (1) initial tension (crimp interchange and yarn pullout) and (2) yarn migration, separation, and fabric shearing at the crossover regions. As the projectile continues to deflect the fabric plane, the leading edge creates an opening between yarn families and, finally, penetration occurs through the opening. The work done by yarn pullout, migration and separation during impact is equal to the energy absorbed by the fabric. Because energy is conserved, the work done by the fabric is equal to the change in kinetic energy of the projectile.

The energy absorbed by the fabric is equal to the change in kinetic energy of the projectile, which is readily computed if the residual projectile velocity is known. Part of the kinetic energy of the projectile is absorbed by the initial tension and deflection of the fabric plane. The majority of the energy, however, is absorbed by the separation and migration of the yarns in the pullout and migration processes. Note that, as the projectile creates an opening within the fabric, both the HCC (warp direction) and LCC (weft direction) yarns are subjected to pullout and migration forces, as shown in figure 31.

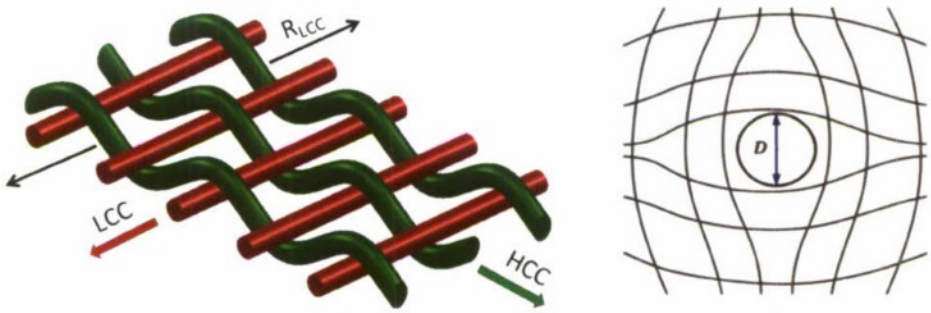

Figure 31. Pullout and Migration Forces in Both HCC and LCC Yarns

For this analysis, consider a swatch of plain-woven fabric—consisting of n x n number of crossover regions—that is impacted by a projectile (see figure 32).

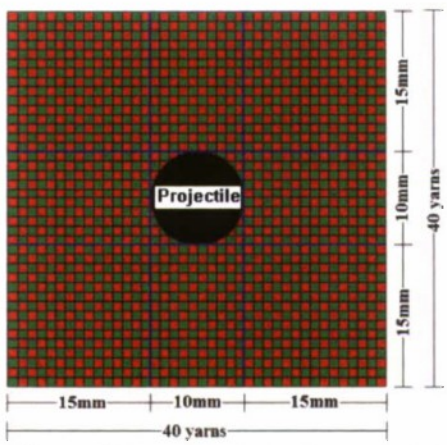

Figure 32. Plain-Woven Fabric Impacted by Projectile with n x n Number of Crossover Regions

To quantify the residual velocity of the projectile, V_2, the following assumptions were made:

- The fabric architecture is plain-woven.
- The yarns have a circular cross section with diameter D equal to 1.0 mm.
- The yarn-to-yarn coefficient of friction is $\mu = 0.1$ to 0.4.
- The angle α varies from 30° to 120° for HCC (as α_x) and from 30° to 60° for LCC (as α_y).
- The tension at the clamped side of the fabric is $T_n = 100$ to 500 N.
- The projectile diameter D is 10 mm.
- The weight of the projectile is 10 g.
- The initial velocity of the projectile was $V_1 = 300$ m/sec.
- The fabric swatch consists of n x n yarns.
- The total area of the fabric swatch is L x L.
- The fabric edges are clamped.
- Yarn compactions at the crossover regions and cross-sectional changes are negligible.
- In the HCC direction, the LCC yarns are separated by distance h (mm), center-to-center of the LCC yarns.
- In the LCC direction, the HCC yarns are separated by distance t (mm), center-to-center of the HCC yarns.
- The HCC yarn direction is X (warp); subscript x represents HCC.
- The LCC yarn direction is Y (weft); subscript y represents LCC.
- Heat generations resulting from yarn-to-yarn and projectile-to-yarn contacts are neglected.
- Crimp contents in the HCC direction and LCC direction are denoted as $\alpha_x = \alpha_{HCC}$ and $\alpha_y = \alpha_{LCC}$, respectively; therefore, crimp imbalance is defined as

  $$\alpha_z = \alpha \frac{\alpha_x}{\alpha_y} = \frac{\alpha_{HCC}}{\alpha_{LCC}} > 1.$$

- The yarns do not fail during the impact event.

Assume that the HCC yarns migrate outward from the impact zone by D_x and are pulled out along the x-direction by amount Δ_x; likewise, assume that the LCC yarns migrate outward from the impact zone by D_y and are pulled out along the y-direction by amount Δ_y. The work W required to create an opening within the n x n plain-woven fabric is equal to the work done by the pullout and migration forces in the x- and y-directions through distances D_x and Δ_x and D_y and Δ_y (see equation (28)).

$$W = \left(R_x D_x + R_y D_y\right) + 2n\left(T_{1x}\Delta_x + T_{1y}\Delta_y\right). \tag{28}$$

Strain energies and heat generation due to yarn-yarn and projectile-yarn contacts were intentionally not included in this study. Thus, the work done by yarn pullout and yarn migration was equated to the change in kinetic energy of the projectile, which was used to compute the residual velocity V_2 of the projectile, as shown in equation (29).

$$W = \frac{1}{2} m\left(V_2^2 - V_1^2\right). \tag{29}$$

RESULTS

To quantify the residual velocity of a projectile, the following example is considered. Consider a plain-woven swatch of a fabric containing 8 x 8 yarns as shown in figure 28. Because the range of α_x is different from the range of α_y, the ratio of the two angles is defined as $\alpha_z = \frac{\alpha_x}{\alpha_y}$. The total work done by the pullout and migration forces, as functions of α_z and different values of tension T_5 (the tension at the swatch edge), is shown in figure 33.

Finally, the projectile residual velocity V_2 is shown in figure 34. As this figure shows, V_2 decreases when the angle $\alpha_z = \frac{\alpha_x}{\alpha_y}$ is increased; that is, increased crimp content of the HCC yarns results in greater energy absorption leading to improved ballistic protection levels of the fabric.

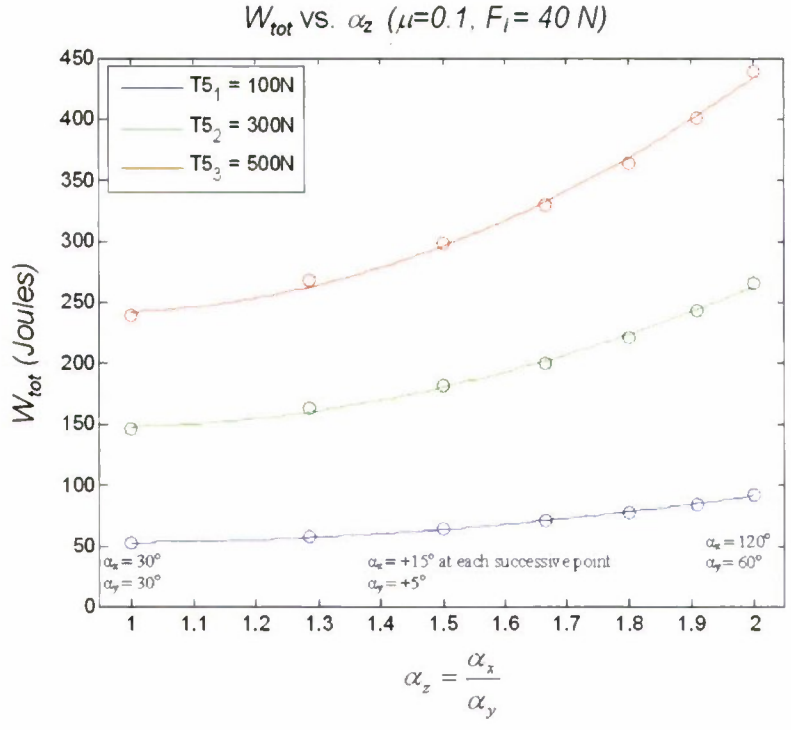

Figure 33. Total Work Done by Pullout and Migration Forces $\alpha_z = \frac{\alpha_x}{\alpha_y}$ for Different Values of T_5

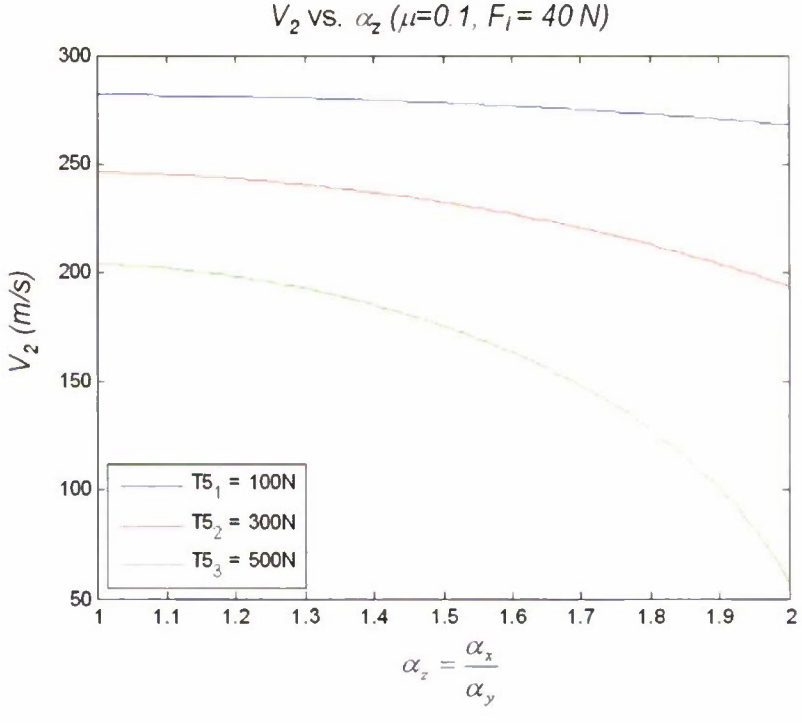

Figure 34. Projectile Residual Velocity V_2 As a Function of $\alpha_z = \frac{\alpha_x}{\alpha_y}$ for Different Values of T_5

SUMMARY AND CONCLUSIONS

Plain-woven fabrics have traditionally been utilized in flexible protection systems because of their combined lightweight and high-strength characteristics. Furthermore, their heterogeneous constructions provide multiple energy absorption mechanisms present at both the yarn and fabric scales enabling them to efficiently and uniquely resist ballistic impacts. The primary objective of this research was to analytically investigate and quantify the hypothesis that plain-woven fabrics constructed with higher crimp contents in one yarn family and lesser crimp contents along the orthogonal yarn family can achieve greater ballistic impact energy absorption. More specifically, this study investigated the mechanisms of projectile penetration into plain-woven fabrics and has developed an analytical solution that quantifies (1) the tensile forces generated by yarn pullout, (2) the frictional forces generated by yarn migration, (3) the work required to create an opening in the fabric, and (4) the residual velocity of the projectile.

In this report, yarn-to-yarn friction at a crossover region was analyzed. When the projectile makes contact with the fabric, a number of crossover regions are subjected to compressive loads. Two types of distributed loading were considered, namely uniform and cosine-shaped. For each case, the ratio of input/output (T_1/T_4) was analytically derived. The results revealed that tension T_1 could exceed 3.5 times that of T_4. This increase was even greater for the cosine-shaped load distribution. In addition, it was found that an increase in the contact angle also increases the (T_1/T_4) ratio. The results indicated that the yarn-to-yarn friction plays an important role in dissipating the kinetic energy of the projectile. Note that, in all the analyses presented in this report, the fibers were assumed to have a high modulus of elasticity; thus the elastic strain of the yarn was neglected.

The architecture of plain-woven fabrics was also studied. The distance between the centerline of two adjacent yarns at crossover regions as a function of contact angle α was analyzed. The results established that angle α sharply increased as h and t, the two distances between adjacent yarns in HCC and LCC directions, respectively, were decreased.

Two mechanisms of energy absorbability present in woven fabrics that are subject to low-velocity ballistic impact are yarn pullout and yarn migration. In this report, yarn pullout forces (T), for cases with and without the projectile forces, were derived. The results reveal that the ratio of yarn tensions (T_1/T_n), at both ends of n number of crossover regions, exponentially increased with an increase in the coefficient of friction μ, angle α, and the number of crossover regions.

By using a realistic example with a projectile velocity of 300 m/sec and a projectile weight of 10 g, the range of impact force F_i was approximated to be between 4500 to 9000 N, depending on the deflection of the fabric (5 to 10 cm for a fabric dimension of 1 x 1 m^2). For this example, the range of tension T_{ni} at the clamped edge was estimated to be between 100 to 500 N. The ranges of F_i and T_{ni} were used for the calculations of the yarn pullout and yarn migration forces studied in this report. The results of the pullout analysis reveal that, for a given T_{ni}, as angle α increases, the tension exponentially increases.

In addition to the yarn pullout force, the yarn migration forces, R, were studied. This phase of the investigation is particularly salient because it demonstrates the significant effect that projectiles with conical leading edges have on fabric. Specifically, a projectile with a conical leading edge deflects the fabric and, in doing so, causes migrations of the primary yarns away from the impact zone—creating openings that lead to through-penetration. Yarn migration forces, for cases with and without projectile impact, were derived. The results revealed that P, the ratio of R/T_n, similar to the pullout force, exponentially increased with an increase in the coefficient of friction μ, angle α, and the number of crossover regions. The same example used for the pullout analysis was used for the yarn migration force analysis. The results of the migration force analysis revealed that, for a given T_{ni}, as α increased, the migration force exponentially increased.

Plain-woven fabrics can absorb significant kinetic energy from projectile and fragment impacts through a combination of yarn pullout and yarn migration phenomenon. The relationship between the energy absorbed by the yarn migration and the residual velocity of the projectile was developed. It was assumed that the projectile created an opening of diameter D. The work done by yarn pullout and yarn migration for the 2 x 2, 4 x 4, and 8 x 8 plain-woven fabrics was derived. In this study, energy transfer caused by heat, elastic strain energy, plastic strain energy, and material damping was not considered. Thus, the work done by yarn pullout and yarn migration was equated to the change in projectile kinetic energy, which was then used to compute the projectile residual velocity V_2. The results revealed that V_2 decreased with increasing contact angle $\alpha_z = \frac{\alpha_x}{\alpha_y}$; that is, increased crimp content of the HCC yarns increased the energy absorption level of the fabric. Finally, the results of this investigation confirmed that fabrics with high crimp contents absorb greater ballistic impact energies than do fabrics with low crimp contents.

Based on the results of this analysis, the following conclusions are provided:

1. As the crimp content and yarn-to-yarn contact angle α of the crossover regions increased, the work done by the projectile on the woven fabric increased, which led to smaller values of V_2. Note that the magnitude of α constituted the crimp content in a given yarn direction.

2. The residual velocity V_2 of the projectile decreased with increased α.

3. The analyses revealed that fabrics with high crimp contents (that is, larger α) absorbed more impact energy than did a fabric with low crimp contents.

These conclusions have been confirmed by the numerical analysis reported in NUWC-NPT Technical Report 11,957.[1] Future experimental tests will be pursued for validation of the analyses performed.

REFERENCES

1. P. Cavallaro and A. Sadegh, "Crimp-Imbalanced Protective (CRIMP) Fabrics," NUWC-NPT Technical Report 11,957, Naval Undersea Warfare Center Division, Newport, RI, 31 March 2010.

2. B. A. Cheeseman and T. A. Bogetti, "Ballistic Impact into Fabric and Compliant-Composite Laminates," *Composite Structures*," vol. 66, pp. 161 – 173, 2003.

3. R. Park and J. Jeng, "Effect of Laminate Geometry on Impact Performance of Aramid Fiber/Polyethylene Fiber Hybrid Composites," *Journal of Applied Polymer Science*, vol. 75, pp. 952 – 959, 2000.

4. D. Roylance, A. Wilde, and G. Tocci, "Ballistic Impact of Textile Structures," *Textile Research Journal*, vol. 43, pp. 34 – 41, 1973.

5. D. J. Carr, "Failure Mechanism of Yarns Subjected to Ballistic Impact," *Journal of Materials Science Letters*, vol. 18, no. 7, pp. 585 –588, April 1999.

6. M. J. Jacob and J. L. Van Dingenen, "Ballistic Protection Mechanisms in Personal Armour," *Journal of Materials Science*, vol. 36, pp. 3137 – 3142, 2001.

7. B. J. Briscoe and F. Motamedi, "The Ballistic Impact Characteristics of Aramid Fabrics: The Influence of Interface Friction," *Wear*, vol. 158, pp. 229 – 247, 1992.

8. Y. S. Lee, E. D. Wetzel, and N. J. Wagner, "The Ballistic Impact Characteristics of Kevlar Woven Fabrics Impregnated with a Colloidal Shear Thickening Fluid," *Journal of Materials Science*, vol. 38, pp. 2825 – 2833, 2003.

9. L. Dischler, T. T. Moyer, and J. B. Henson, "Dilatant Powder Coated Fabric and Containment Articles Formed There," U.S. Patent 5,776,839, 1998.

10. J. Awerbuch and S. R. Bodner, "Analysis of the Mechanics of Perforation of Projectiles in Metallic Plates," *International Journal of Solids and Structures*, vol. 10, pp. 671 – 684, 1974.

11. S. A. Sebastian, A. I. Bailey, B. J. Briscoe, and D. Tabor, "Effect of a Softening Agent on Yarn Pull-Out Force of a Plain Weave Fabric," *Textile Research Journal*, vol. 56, pp. 604 – 611, 1986.

12. S. A. Sebastian, A. I. Bailey, B. J. Briscoe, and D. Tabor, "Extensions, Displacements, and Forces Associated with Pulling a Single Yarn From a Fabric," *Journal of Physics D: Applied Physics*, vol. 20, pp. 130 – 139, 1987.

13. F. Motamedi, A. I. Bailey, B. J. Briscoe, and J. Tabor, "Theory and Practice of Localized Fabric Deformations," *Textile Research Journal*, vol. 59, pp. 160 – 172, 1989.

14. M. A. Martinez, C. Navarro, R. Cortes, J. Rodriguez, and V. Sanchez-Galvez, "Friction and Wear Behaviour of Kevlar Fabrics," *Journal of Materials Science*, vol. 28, pp. 1305 – 1311, 1993.

15. S. Bazhenov, "Dissipation of Energy by Bulletproof Aramid Fabric," *Journal of Materials Science*, vol. 32, pp. 4167 – 4173, 1997.

16. D. A. Shockey, D. C. Erlich, and J. W. Simons, "Improved Barriers to Turbine Engine Fragments: Interim Report III," DOT/FAA/AR-99/8, III, Office of Aviation Research, Federal Aviation Administration, Washington, DC 2001.

INITIAL DISTRIBUTION LIST

Addressee	No. of Copies
U.S. Army Research Laboratory, Aberdeen Proving Ground, MD (AMSRD-ARL-WM-MD (B. Cheeseman (5), R. Dooley, C. Yen, B. Scott, D. Granville), RDRL-WMM-D (V. Champagne, Jr.), RDRL-WMP-F (A. Frydman), RDRL-WMM-A (M. Maher))	12
U.S. Army Aberdeen Test Center, Aberdeen Proving Ground, MD (TEDT-AT-WFT (F. Carlen))	1
U.S. Army Natick Soldier Research, Development, and Engineering Center, Natick, MA (M. Jee, F. Kostka, J. Hampel, C. Quigley, K. Horak, P. Cunniff, J. Ward, J. Mackiewicz, D. Lee, T. Godfrey, R. Benny, G. Thibault)	12
U.S. Army Research Office (RDRL-RO-EN (B. LaMattina, D. Stepp, W. Mullins))	3
Navy Clothing and Textile Research Facility, Natick, MA (B. Avellini, L. Caulfield, T. Hart, C. Heath)	4
Naval Surface Warfare Center, Panama City, FL (Code CX05 (F. Garcia))	1
Naval Surface Warfare Center, Carderock Division, W. Bethesda, MD (Code 65 (R. Crane, E. Rasmussen), Code 664 (P. Dudt))	3
Naval Surface Warfare Center, Dahlgren Division, Dahlgren, VA (Code G25 (W. Mock))	1
Office of Naval Research (ONR-DOI (L. Schuette), ONR-331 (R. Barsoum), ONR-334 (Y. Rajapakse))	3
Weapons and Protective Systems COE, Applied Research Laboratory/ Pennsylvania State University	1
Savannah River Site (J. Wong, C. Robinson)	2
Warwick Mills, New Ipswich, NH (C. Howland)	5
Defense Technical Information Center	2
Center for Naval Analyses	1